

Gas Sensor by Using Semi conducting Porous Nan Crystalline Silicon

**A Major Project Submitted in the Partial Fulfillment of the
Requirement for the Degree of
MASTER OF ENGINEERING
In
POLYMER TECHNOLOGY**

**in the Faculty of Technology,
University of Delhi, Delhi**

**Submitted By
S.CHANDRA MOHAN**

Under the Guidance of

Dr. D.Kumar

&

Dr. S.N. Sharma



**DEPARTMENT OF APPLIED CHEMISTRY
AND POLYMER TECHNOLOGY
DELHI COLLEGE OF ENGINEERING
DELHI - 110042**

Dedicated to
My Father
(Shri. S. Lakshmi Narayana)

And

My Mother
(Smt. S. Symala Devi)

CERTIFICATE

This is to certify that the project entitled “**gas sensor by using Semiconducting porous nanocrystalline silicon**” completed by **Mr. S. Chandra Mohan**, student of **Master of Engineering** (Polymer technology) from Delhi College of Engineering, Delhi embodies the original work carried out by him under the joint supervision of Dr. D.Kumar, Assistant professor, Department of Applied chemistry, Delhi College of Engineering, Delhi and Dr.S.N.Sharma, scientist, Electronics Material Division, National Physical Laboratory (N.P.L), New Delhi.

His work has been found excellent for the partial fulfillment of the requirement of the degree of M.E. It is further certified that, the student has developed the project with the help of nanomaterial Professionals in the N.P.L, New Delhi during the period starting from 1st of October to 30th June 2005.

This Report has not been submitted in part or full in any other University for award of any degree or diploma.

Dr.G.L.Verma,

(Dr .D. Kumar)
Supervisor

Endorsement No: _____

Dr.S.K.Chakladar,

(Dr. S.N. Sharma)
Co-Supervisor

ACKNOWLEDGEMENTS

It is my pleasure to take this opportunity to express my heartfelt gratitude Dr. D. Kumar, Assistant professor, Department of Applied Chemistry, Delhi College of Engineering under whose able guidance and supervision this research work has been carried out .It would not have been possible for me submit this research work, without his critical suggestions, constant inspiration and timely help.

It is my pleasure to take this opportunity to express my heartfelt gratitude to my co-supervisor Dr. S.N. Sharma for his kind support, advice, and guidance throughout my M.E research. I am very grateful to Dr. S.N. Sharma for introducing me to the area of semi conducting materials and fostering an atmosphere of openness, creativity and encouragement throughout my M.E research at Electronic Materials Division, National Physical Laboratory, New Delhi, India.

I am grateful to Dr. P.V. Sharma, Principal and Dr.G.L. Varma, Head, Department of Applied Chemistry of Delhi College of Engineering, Delhi, for providing me the necessary facilities and required co-operation during the tenure of my experimental work.

I am highly thankful to Prof. Vikram Kumar, Director, National Physical Laboratory, New Delhi for extending all facilities to pursue the research work.

I express my gratitude to Dr. S.K. Chakladhar Head, HRM, Dr. S.N. Singh Head, Materials Division and Dr. S.T. Lakshmi Kumar, Electronic Materials Division, National Physical Laboratory, New Delhi.

Finally, this research can never be completed without continuous support of my both sisters Vijaya Lakhmi and Krishna Priya for their love and enthusiastic support throughout the research.

At last but not the least, I am grateful to all those who have directly or indirectly helped me during the period of this research work.

Dated:

(S. Chandra Mohan)

PREFACE

This Project demonstrates the studies of semiconducting nanocrystalline thin films for sensing applications using electrochemical and vacuum deposition method. These semiconducting porous silicon thin films sensors incorporate metal/ PS /metal junction with electro chemical synthesized porous silicon. This Project concentrates on the study of semiconducting porous silicon thin films. The electrical characteristics of these semiconducting porous silicon thin films were studied of their application to prepare gas sensor for detection of hazardous gases.

Recently the environmental protection policy of most of the industrially developing countries is oriented towards the regulation, monitoring and control of hazardous gases in the atmosphere and biological activity. An increasing public concern towards pollution control and cleaner environment has, therefore, putting a greater demand for better and cheaper materials and devices for detection of toxic gases. The available devices are based on solid-state inorganic semiconducting sensor elements where in the detection is carried out by measurement of conductance changes due to gas adsorbed (chemisorption) onto the material surface. Tin-oxide based thin film sensors have been fabricated by a variety of techniques such as spray pyrolysis, chemical vapors deposition, electron beam evaporation and sputtering. However, with these techniques, it is sometimes difficult to add additives (dopants and catalysts) uniformly into the thin film. A recent technique, known as vacuum deposition, has been found to have several advantages, such as excellent homogeneity, simple, low cost, and dry processing etc, the most significant advantage of the process is the ability to produce large surface area powders and films, which result in increased sensitivity.

Semiconducting metal oxide based gas sensors generally operate efficiently at 250°C or above. In order to overcome this limitation new materials are being attempted at our laboratory. Recently, electro-active conductive

polymers such as appropriately doped polypyrrole; polythiophene and polyaniline have emerged as efficient gas sensors. Conducting polymers such as polypyrrole and polyaniline have recently attracted much attention. These interesting molecular electronics materials have been considered to have potential application in electro-optical devices, batteries and molecular electronics etc. It has been thought that the detailed information with regards to the optical and electrical properties holds the key towards the commercialization of those important conduction materials.

The present work deals with a description of the fabrication of semiconducting materials thin film devices-sensor materials utilizing vacuum deposition techniques. It has been observed that sensitivity; selectivity, optimum operating temperature and response time of the gas sensing elements depend, in a complex manner, on the dopants and additives.

This film has been synthesized using electrochemical and vacuum deposition technique respectively. Optical and electrical properties of various thin films have been experimentally investigated. Various junction parameters such as ideality factor, barrier height, and carrier concentration etc., of the Schottky diode based on semiconducting thin films have also been determined. It has been observed that vacuum deposited thin films of material exhibit excellent gas sensing properties. The electrical conductivity, optical absorption and electrical capacitance of metal/nanocrystalline interface are strongly influenced by the presence of gas molecules. These results have led to the development of sensors for toxic gases. The thin film based gas sensors are inexpensive and are operated at room temperatures with satisfactory selectivity for these gases. Efforts are being made to understand the basic mechanism of gas sensing behavior of such semiconducting nanocrystalline thin films.

LIST OF FIGURES

Page no: -

Fig.1.1 Sensor system	5
Fig.1.2 Classification of sensor according to the principal of operation	5
Fig.1.3 FTIR	3
Fig.1.4 Scanning electron micrographs of porous silicon prepared on textured substrates at $I_d = 35 \text{ mA cm}^{-2}$; a) Electrolyte HF: Ethanol, b) HF: H_2O_2	10
Fig:1.5 Schematic diagram of a combined scanning electron microscope analyzer	10
Fig:2.1 Mechanism of Forming PS	19
Fig.2.2 different conducting polymers	19
Fig:3.1 - Block diagram for preparation of gas sensor	34
Fig.3.2 Electrochemical anodization a) Single tank Cell b) Double tank Cell	37
Fig.3.3 Porosity of PS as a function of current density (I_d); (a) Textured substrate, Electrolyte B; (b) Polished substrate, Electrolyte B; (c) Textured substrate, Electrolyte A; (d) Polished substrate, Electrolyte A.	42
Fig: 3.4 –Mechanism of Forming PS	46
Fig.4.1 Scanning electron micrographs of porous silicon prepared on polished substrates at different current densities (I_d); (a) $I_d = 10 \text{ mA cm}^{-2}$, Electrolyte A; (b) $I_d = 10 \text{ mA cm}^{-2}$, Electrolyte B; (c) $I_d = 35 \text{ mA cm}^{-2}$, Electrolyte A; (d) $I_d = 35 \text{ mA cm}^{-2}$, Electrolyte B.	50
Fig.4.2 The AFM image of the textured porous silicon surface shows large (100 nm) size pores at some regions. This is not seen in textured silicon or in porous silicon formed on polished silicon substrates	51
Fig.4.3 PL spectra of porous silicon samples prepared at different current densities (I_d) for (A) electrolyte A and (B) electrolyte B; (a) Textured substrate, $I_d = 20 \text{ mA cm}^{-2}$; (b) Polished substrate, $I_d = 20 \text{ mA cm}^{-2}$; (c) Textured substrate, $I_d = 35 \text{ mA cm}^{-2}$; (d) Polished substrate, $I_d = 35 \text{ mA cm}^{-2}$ (e) Textured substrate, $I_d = 50 \text{ mA cm}^{-2}$ and (f) Polished substrate, $I_d = 50 \text{ mA cm}^{-2}$.	53

Fig.4.4 PL spectra of porous silicon samples prepared at different current densities (I_d) for (A) electrolyte A and (B) electrolyte B; (a) Textured substrate, $I_d = 20 \text{ mA cm}^{-2}$; (b) Polished substrate, $I_d = 20 \text{ mA cm}^{-2}$; (c) Textured substrate, $I_d = 35 \text{ mA cm}^{-2}$; (d) Polished substrate, $I_d = 35 \text{ mA cm}^{-2}$ (e) Textured substrate, $I_d = 50 \text{ mA cm}^{-2}$ and (f) Polished substrate, $I_d = 50 \text{ mA cm}^{-2}$.	54
Fig:4.5 FTIR absorption spectra of porous silicon prepared at current density $I_d = 20 \text{ mA cm}^{-2}$; (a) Textured substrate, Electrolyte A; (b) Polished substrate, Electrolyte A; (c) Textured substrate, Electrolyte B; (d) Polished substrate, Electrolyte B.	58
Fig .4.6 Block diagram of gas detector circuit	60
Fig.4.7 Total diagram of gas sensor.	62
Fig.5.1 PL spectra of porous silicon sample exposed at different gasses	65
Fig.5.2 FTIR transmission spectra of porous silicon prepared at current density $I_d = 20 \text{ mA cm}^{-2}$; (a) as made PS and Humidity Exposed.	67
Fig.5.3 FTIR transmission spectra of porous silicon prepared at current density $I_d = 20 \text{ mA cm}^{-2}$; before coated and after coated with polymer	68

LIST OF TABLES

Table: 3.1 - Specification for Electrochemical method	38
Table: 3.2 - Effects of Electrochemical method and conditions	40
Table: 3.3 - types of PS according to porosity	43
Table: 3.4- Electrochemical method for coating PPY on Porous Silicon	48
Table: 4.1-Peak Positions of Surface Species by FTIR method	56
Table: 4.2-specification for gas sensor	63
Table: 5.1-Calculating change of resistance and resistivity as prepared and after exposed.	69

CONTENTS

	Page No.
Organization Certificate	i
Acknowledgements	ii
Preface	iii
List of figures	v
List of tables	vi
Contents	vii

CHAPTER-1

1. Introductions	1
1.1 Introduction about Project	2
1.2 Applications using ps based semiconducting nanomaterials	3
1.3 Sensors	4
1.4 Classifications of sensors	6
1.5 electro luminescent devices	7
1.6 characterization techniques for semiconducting nanomaterials	7
1.6.1 FTIR	7
1.6.2 Photoluminescence	8
1.6.3 Scanning electron microscopy (SEM)	8
1.6.4 Atomic force microscope (AEM)	8
1.6.5 Current – voltage (I-V) measurements	11
1.7 Vacuum pumping systems:	11

CHAPTER - 2

2. Studies on material	15
2.1 Dissolution chemistry	16
2.2 Properties.	16
2.3 Preparations	17
2.4 Structures	17
2.5 Formation of porous silicon	18
2.6 Conducting polymer	20
2.7 Semiconducting polymers	20
2.8 Advantages of semiconductors conjugated molecules	22
2.9 Doping of conjugated polymers	22
2.10 Study on polypyrrole	23
2.11 Different methods for preparation of semiconducting polymer films	25
2.11.1 Vacuum deposition	
2.11.2 Langmuir – Blodgett (LB) film deposition	
2.11.3 Spin coating	
2.11.4 Dip coating	
2.11.5 Electrochemical polymerization	
2.11.6 Sol-gel method	
2.11.7 Physical method	
2.11.8 Sputtering chemical method	
2.12 Preparation of pani, ppy & co-polymer films	30

CHAPTER – 3

3. Experimental	31
3.1 Introduction	32
3.2 Materials	33
3.4 Synthesis of semiconducting porous nanocrystalline silicon	33
3.5 Electrochemical formation	35
3.6 pore formation	39
3.7 Effect of anodization conditions	39

3.8 Different types of ps	42
3.9 Formation of porous silicon	43
3.10 Drying of the samples	47
3.11 polymer coated porous silicon	47

CHAPTER – 4

4. Electrical and optical characterization	49
4.1 morphology of the resulting layers	50
4.2 AFM image of pores	51
4.3 Photoluminescence	52
4.4 FTIR	56
4.5 Sensing materials or contacts for gas sensor	59
4.5.1 Vacuum pumping systems	
4.5.2 Nickel coating:	
4.6 Device fabrication	60
4.7 Energy band diagram analysis	61
4.8 Response time analysis	62
4.9 Specification for gas sensor	63

CHAPTER – 5

5. Results & discussion	64
5.1 Photoluminescence	65
5.2 FTIR	66
5.3 Study of polymer coated porous silicon	68
5.4 Sensitivity	69
5.5 Conclusions	70

CHAPTER - 6

6. Summary	72
7. Reference	75

INTRODUCTION

1.1 INTRODUCTION ABOUT PROJECT

Monitoring and upkeep of the environment, for well being and health carries a very broad area comprise diverse factors like chemical, biological and human habitat. Historically, toxicity in the environment, infections and communicable disease has been at the center of environmental health including physical, sociological and psychological factors that may affect man's health and safety. Identification of toxicity, causative organisms, and routes of transmission, population at risk and the subsequent development of strategies to prevent transmission or treatment and cures for communicable diseases has dominated public health. Today, while chemical and biological hazards continue to be enormous public health issues, other hazards have emerged and demand attention. Concern for presence of chemicals and microorganisms in the atmosphere and their possible effect on human health has attained prominence. Some brief background of pioneering works in the area of PS thin films fabrication and characterization techniques have been presented. Studies performed on PS have revealed that semiconducting PS is stable for about two years. PL and FTIR studies have brought the mode of synthesis and subsequent processing that do not significantly affect the physical characteristics of PS It begins with a description of the sample preparation procedure and it continues with the characterization techniques. For each characterization technique the basic theory is outlined, the setup is described and the measurement procedure is discussed. Accuracy and sensitivity requirements are addressed. It contains all the necessary information for the future repetition of this work. We have also reported morphological, optical and electrical studies of Electrochemical deposited thin film of PS. The results are investigation with PL, FTIR, SEM and AFM.

It can be concluded that quality PS nanocomposite thin films can be prepared by Electrochemical method. These films can be used for as efficient sensors for detection of gas like ethanol, methanol, humidity

etc. These films are nanocrystalline in nature and behave like granular metallic crystallites embedded in a nonconducting medium. High sensitivity specificity and selectivity can be achieved by suitably PS at particular current density during synthesis. A stoichiometric composition of electrolyte HF: Ethanol (1:1). has been found to be suitable for detection of gas. The response time of sensor is very small. The sensor is reusable, as there is no chemical reaction between PS thin film and the gas. The sensor is operated at room temperature and no heating of the sensor materials is required, there the sensor extends lifetime considerably. The behavioral acceptance test indicates that electrochemical deposited PS thin film sensors are most suitable for online detection and continuous monitoring of gas.

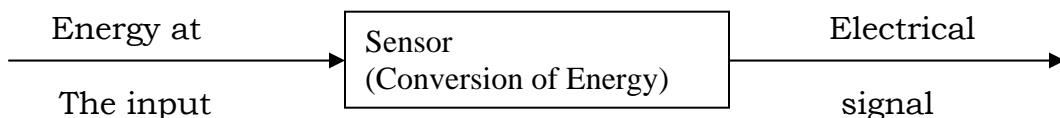
1.2 APPLICATIONS USING PS BASED SEMICONDUCTING NANOMATERIALS

Semiconducting materials are novel materials with potential technological applications. These electronic materials have found various advantages because of the lightweight, ease of processing and economic over traditional metals/semiconductors. These nanomaterials have found their uses in lightweight rechargeable batteries, electrostatic charge dissipation, electromagnetic interference (EMI) shielding, memory devices, nonlinear optics, bioelectrochemistry, sensors, electroluminescent devices, solid-state electronics etc. A brief summary of the some of the application of semiconducting materials reported in literature is given below.

1.3 SENSORS

A sensor is a device having a capable to respond against an externally applied stimulus. Depending upon the nature of the external stimuli, a sensor may either be a gas, chemical or biosensor. Need for accurate real time and quick information in the area like health care, veterinary research, agriculture, chemical industries and pollution control has led to an ever-increasing demand for research and development on sensors. The importance of nanomaterials in sensors arises due to the ease of their ability to incorporate sensing elements in the nanomaterial network. Apart from these properties these materials also exhibit interesting electrical properties such as, their ability to oxidize and reduce at specific electrochemical potential. Besides this, these exhibit semiconducting properties, upon incorporation of suitable dopants.

Sensors become important factors in automation and robot technology and gain an increasingly greater significance as structural elements of system. It may be necessary to linearize the signal. There are two basic types of sensors: active and passive. The active sensor converts one form of energy directly into another without the need for an external source of energy or excitation (Fig.1.1). The passive sensor cannot convert energy directly but it controls the energy on the excitation entering from another source. The sensor carries out a quantitative conversion of a certain property of the substance or the process. The substance may be a solid, a liquid or a gas and its state may be static or dynamic.



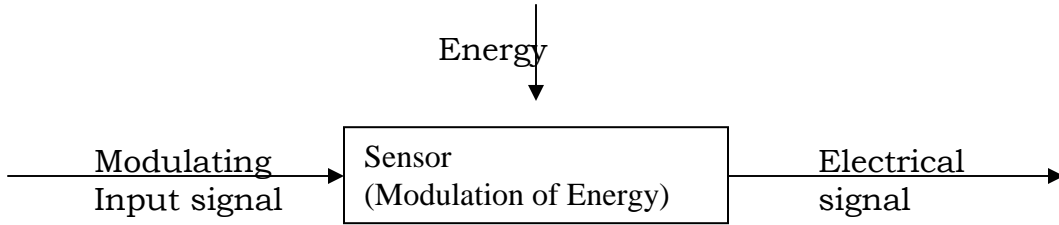


FIG.1.1 Sensor system

1.4 CLASSIFICATIONS OF SENSORS

Sensor can be classified from the point of view of their principles of conversion (the physical and chemical effects on the basis of which they operate), their purpose, the type of output signals, the materials and the technology of their production. The classification of sensors according to their principal of operation is shown in FIG.1.2.

They can be divided into physical and chemical ones. Physical sensors employ physical effect, such as piezoelectric, magnetostrictional, ionization, photoelectric, magneto electric etc. The smallest changes in the quantity being measured are converted into an electrical signal. Chemical sensors include sensors in which, as a result of chemical absorption, electrochemical reactions, etc. the smallest changes in the quantity being measured are converted into an electrical signal.



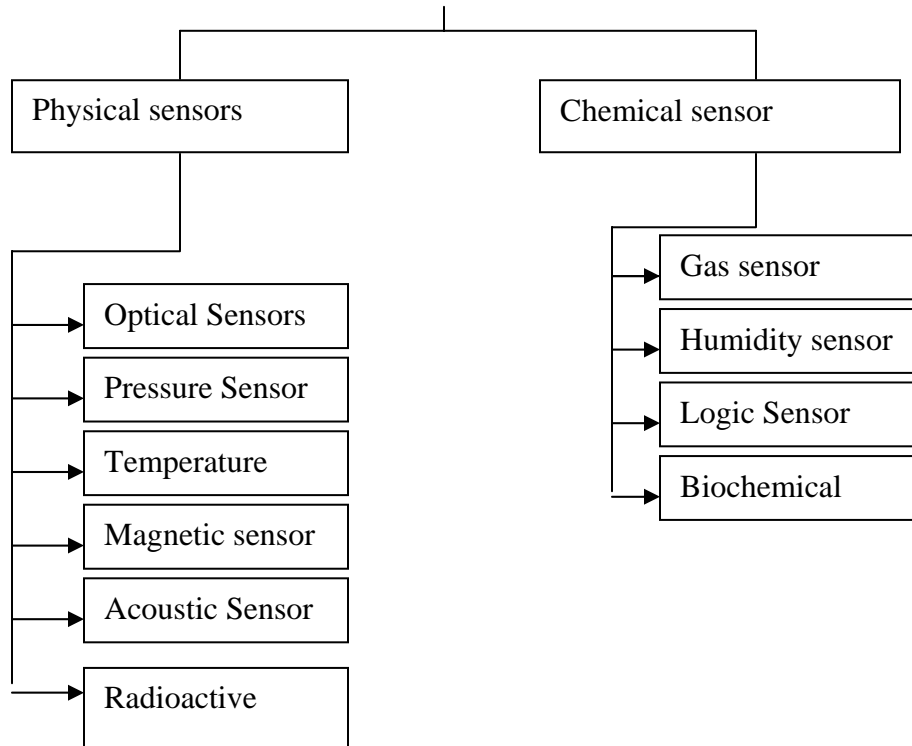


FIG.1.2 Classification of sensor according to the principal of operation

1.5 ELECTROLUMINESCENT DEVICES

The phenomenon of emission of visible light due to applied electric field is called electro luminescence and devices based on it are known as electro luminescent devices. Light emitting diode (LED) is one of the most important electro luminescent devices. Commercially available red color LED made of gallium arsenide operates at 1.5 volts having a quantum yield of about 1%. The quality of an LED is assessed by the efficiency of photoemission and threshold operating voltage. These materials have recently attracted much attention for their use in fabrication of LED.

1.6 CHARACTERIZATION TECHNIQUES FOR SEMICONDUCTING NANO MATERIALS

1.6.1 FOURIER TRANSFORMS INFRARED SPECTROSCOPY (FTIR)

This is an indispensable tool for the structural characterization of any conducting or semi conducting material. The frequencies and intensities of various vibration bands exhibited by a given organic compound unequally characterize the material. FTIR spectra can be used to identify and quantify a particular substance in an unknown sample. Perkin Elmer (Spectrum BX) FTIR spectrophotometer having a spectral rang of $400\text{-}4000\text{ cm}^{-1}$ with 4 cm^{-1} resolution has been used for the characterization of various material in their respective doped and undoped sates using a method of vibration band indexing. FTIR spectra of material in thin film form have been recorded. FTIR spectra of thin transparent electro deposition films of PS on Si substrate have been obtained in reflection mode using a reflectance accessory. Freestanding conducting PS films have been directly used for spectral studies. The FTIR spectrum of polystyrene standard obtained using the Nicolet FTIR spectrometer is shown in (FIG.1.3)

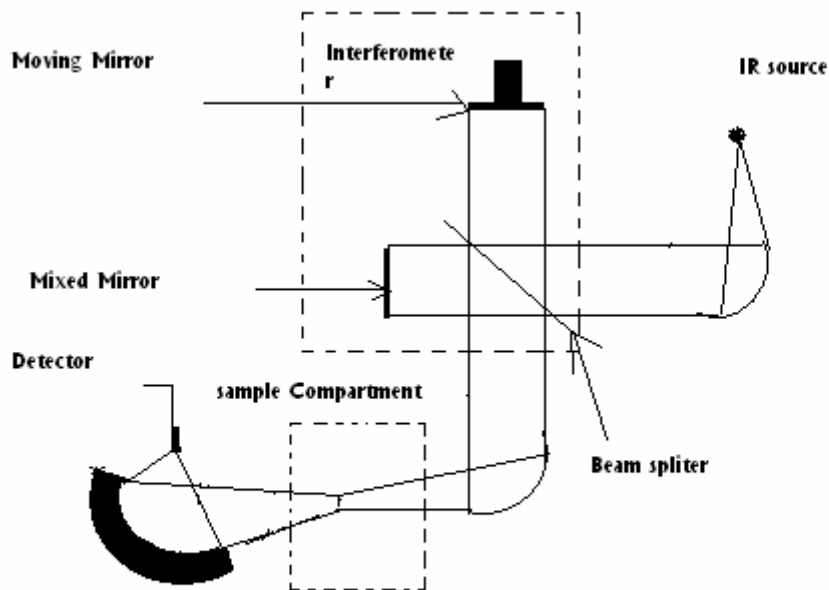


Fig: Schematic diagram of a FTIR spectrometer

1.6.2 PHOTOLUMINESCENCE

The PL was measured using a home assembled system consisting of a two stage monochromator, a photomultiplier tube (PMT) with a lock-in amplifier for PL detection, and an Ar⁺ ion laser operating at 488 nm and 5 mW (corresponding to 0.125 W cm⁻²) for excitation in all the measurements. Decay of PL intensity has been used as a measure of the stability of the surface bond configurations [7]. For PL decay studies, the sample was continuously exposed to the laser radiation and PL measurements were carried out. It has been observed that PL decay in the case of PS films formed on textured substrates is negligible as compared to the corresponding films formed on polished substrates.

1.6.3 SCANNING ELECTRON MICROSCOPY (SEM)

SEM has been widely used for the visualization of organic surfaces especially in the study of surface morphology. SEM technique

uses the intensity of secondary emissions (usually broad energy distribution) of secondary electron. Some of these electrons that recombine with ions at the surface are the basis for the SEM imaging capabilities. The SEM shows very detailed 3-dimensional images at much higher magnifications than is possible with a light microscope. The images created without light waves are rendered black and white. The contrast in the image is result of differences in scattering from different surface areas as a result of geometrical differences.

Principle of operation:

A microscope creates an image of a sample by scanning the sample with a electron beam. Secondary electron are subsequently emitted from the sample, are collected in the microscope detector, and are reconfigured at various magnifications on a cathode ray tube as an image of the sample. Samples have to be prepared carefully to withstand the Vacuum inside the microscope. The sample is placed inside the microscope's vacuum column through an airtight door after the air is pumped out of the column; an electron gun (at the top) emits a beam of high-energy electrons. This beam travels downward through a series of magnetic lenses designed to focus the electrons to a very fine spot. Near the bottom, a set of scanning coils moves the focused beam back and forth across the specimen, row by row. As the electron beam hits each spot on the sample, secondary electrons are knocked loose from its surface. A detector counts these electrons and sends the signals to an amplifier. The final image is built up from the number of electrons emitted from each spot on the sample. The SEM of PS thin film on the glass plate has been shown in the (FIG.1.4)

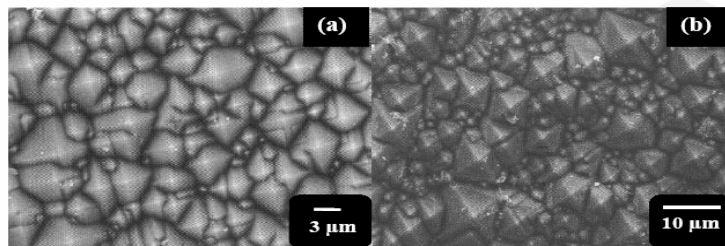


Fig.1.4 Scanning electron micrographs of porous silicon prepared on textured substrates at $I_d = 35 \text{ mA cm}^{-2}$; a) Electrolyte HF: Ethanol, b) HF: H_2O_2

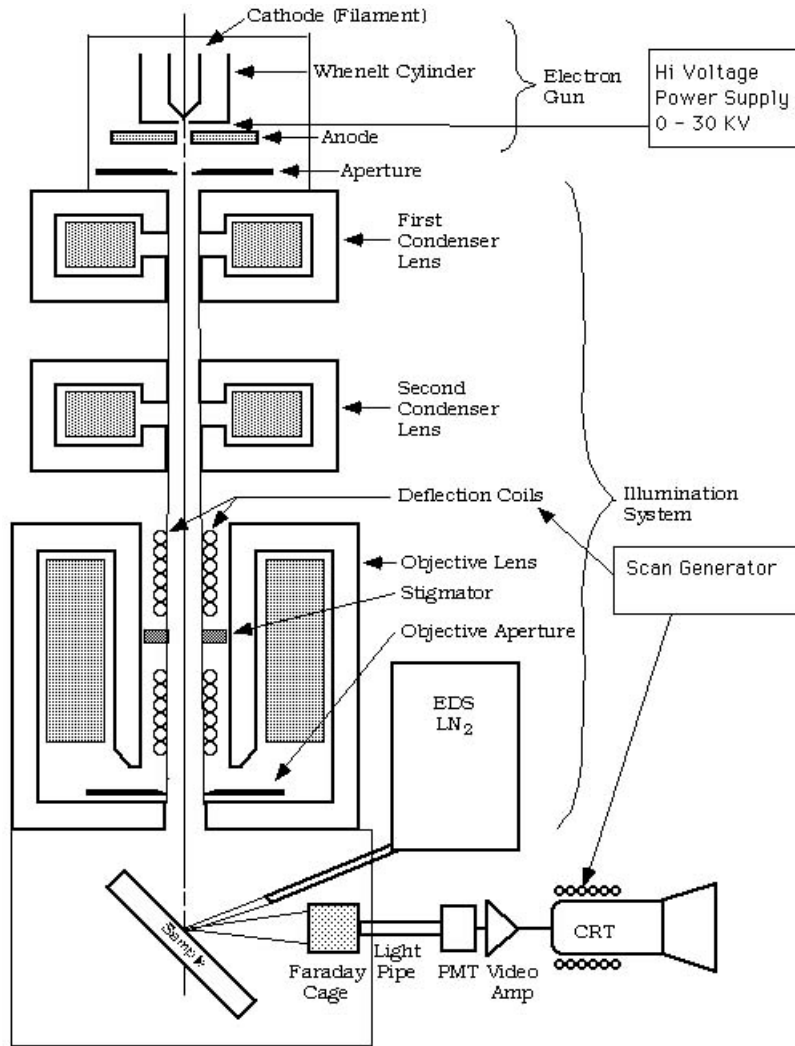


Fig:1.5 Schematic diagram of a combined scanning electron microscope analyzer

1.6.4 ATOMIC FORCE MICROSCOPE (AFM)

An AFM uses a tiny silicon tip, usually less than 100 nm in diameter, as a probe to create an image of a sample material. As the silicon probe moves along the surface of the sample, the electrons of the

atoms in the sample repel the electrons in the probe. The AFM adjusts the height of the probe to keep the force on the sample constant. A sensing mechanism records the up – and down movements of the probe and feeds the data into a computer, which creates a three – dimensional image of the surface of the sample. Thus, the exact surface topography can be recorded with precise height information, and individual atoms in the surface can be imaged. The lateral resolution of this technique, however, is sometimes poor.

1.6.5 CURRENT – VOLTAGE (I-V) MEASUREMENTS

I-V measurements determine the electrical output performance of devices. This measurement technique is an ideal for dc characteristic measurement. Such as, leakage current, current-voltage characteristics and determining dc parameters for semiconductor devices, required by the semiconductor industry for new product development and for improving production yield.

1.7 VACUUM PUMPING SYSTEMS:

The HINDHIVAC combined high vacuum pumping systems are used for our sensing material. These systems give an ultimate vacuum of 10^{-5} m.bar or better. In our case we are using Model VS-114. To achieve better ultimate vacuum the system the system should incorporate suitable traps like foreline trap, liquid nitrogen cold trap or chevron baffle as per the requirement. Our system is water-cooled type. They can be connected for creating vacuum in laboratory systems, lamp manufacturing units, T.V.tubes manufacturing, X-ray, distillation plants, and vacuum furnaces etc.

1.7.1 GENERAL DESCRIPTION

The diffusion pump and Rotary pump with accessories are mounted within the frame the vacuum gauges which are also placed in the frame, or can be placed at any convenient position desired by the operator. The oil diffusion pump is fixed at the top of the frame while the rotary pump is fitted at the bottom of the frame. The diffusion pump used here is either fractionating or non fractionating, water-cooled type. A water cooled baffle valve is fitted above the diffusion pump over which is a vacuum collar is installed with necessary ports for connecting the vacuum gauge heads, air admittance valve etc. An air admittance valve of suitable size and a fine control type needle valve for inert gas respectively are provided. The system to be evacuated can be directly connected to the vacuum collar with the use of the suitable adapter. The top of the collar is closed with a dummy plate, which can be removed, and a base plate can be fixed in place of it. Necessary feed-through can be introduced through the based plate to use the system for any other application like evaporation etc. with a bell jar and necessary gadgets. Water cooled chevron baffle will be fitted in between the diffusion pump and high vacuum valve to attain clean and ultimate vacuum, in case of specified orders only. Stainless steel pipelines are used for roughing and backing purposes, with isolation valves/quarter swing type butterfly valves of suitable size, for convenient isolation of the diffusion pump from the system whenever roughing operations are going on. The pirani-penning gauge system is provided with two Pirani gauge heads fitted in backing and roughing lines to read the corresponding vacuum and one penning gauge head fitted to the collar to read high vacuum. As such the gauge system operates in the vacuum range of 0.5 to 10^{-6} m.bar.

1.7.2 PARTS OF VACUUM PUMP

1. Main frame
2. Rotary vacuum pump
3. Diffusion pump. Baffle valve and liquid air/nitrogen trap
4. Gauges (Pirani & Penning gauges).
5. Pipelines pump fluids and other accessories.

1.7.3 OPERATION

1. Switch on the rotary pump by pressing the rotary pump start switch or circuit breaker on the control panel.
2. Open the backing valve slowly keeping roughing and other valve closed and observe the reading in Pirani gauge by selecting gauge heads 1
3. As soon as the Pirani gauge shows a vacuum better than 0.5 m.bar, switch on the diffusion pump by selecting the diffusion pump start switch or circuit breaker on the front panel. Make sure that water connections are given to the diffusion pump cooling line. The diffusion pump takes about 30 minutes to attain the operating temperature.
 1. Close the backing valve and slowly open the roughing valve. Select gauge head 2 in the Pirani gauge to read the roughing vacuum. When the vacuum in the collar reaches better than 0.05 m.bar close the roughing valve and slowly open the backing valve. Now the system is ready to test for high vacuum.
 2. Open the baffle valve slowly without applying much force. Now pointer in the gauge moves to right.
 3. Switch on the Penning gauge and select the range. The pointers will now show the exact vacuum in the collar.

1.7.4 SHUT DOWN OF THE SYSTEM

It is recommended to leave the chamber under vacuum. This reduces pump down time and leaves the system clean.

1. Switch off the Penning gauge.
2. Close the baffle valve slowly without applying much force.
3. Close the roughing valve
4. Keep rotary pump running for about 30 minutes and then close the backing valve and switch off the diffusion pump heater.
5. Switch off the Pirani gauge.
6. Allow the water flow for some time to cool the diffusion pump and then close the water connection.
- 7.** Switch off the Rotary pump.

CHAPTER 2

STUDIES ON MATERIALS

2.1 DISSOLUTION CHEMISTRIES SILICON

It is found in free state in sand & quartz.

Feldspar $K_2O, Al_2O_3, 6SiO_2$

Keolinite $Al_2O_3, 2SiO_2, 2H_2O$

Asbestor cao $3MgO, 4SiO_2$

Silicon is second member of group 14 of the periodic table. Its electronic configuration is $1S^2 2S^2 2P^6 3S^2 3P_x^1 3P_y^1$, like carbon, silicon has four valence electrons. Silicon forms covalent compounds like SiH_4 and SiX_4 (X=halogens) just in the same way as carbon forms CH_4 and CX_4 . Both silicon and carbon show tetra covalence in the above compounds. Silicon like carbon has tetrahedral geometry in the compounds.

2.2 PROPERTIES.

Large size of silicon atom: The size of silicon atom (117 pm) much larger than carbon (77 pm) and other. As a result, Si -O bonds are much stronger than Si-Si and Si - H bonds.

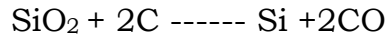
Electronegativity: The electro negativity of silicon (1.9) is less than that of carbon (2.5).

Multiple bonding: Due to the larger atomic size and lower electro negativity, silicon does not form a $p\pi -p\pi$ double bond with itself or with oxygen.

Availability of d - orbital: Silicon has vacant 3d-orbitals in its valence shell and hence can utilize these orbital for bonding. As a result, silicon can extend covalence from four to five and six.

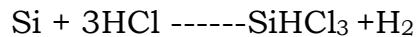
2.3 PREPARATION:

The raw feedstock for Si crystal is silicon dioxide (SiO₂), we react SiO₂ with C in the form of coke in an arc furnace at very high temperatures (1800°C) to reduce SiO₂ according to the following reaction:



This forms metallurgical grade Si (MGS) which has impurities such as Fe, Al and heavy metals at levels of several hundred to several thousand parts per million (ppm). That one-ppm of Si corresponds to an impurity level of $5 \times 10^{16} \text{ cm}^{-3}$. While MGS is clean enough for metallurgical applications such as using Si to make stainless steel, it is not pure enough for electronic applications; it is also not single-crystal.

The MGS is refined further to yield semiconductor-grade or electronic grade Si (EGS), in which the levels of impurities are reduced to parts per billion or PPB (1 PPB = $5 \times 10^{13} \text{ cm}^{-3}$). This involves reacting the MGS with dry HCl according to the following reaction to form trichlorosilane, SiHCl₃, which is a liquid with a boiling point of 32°C.



Along with SiHCl₃, chlorides of impurities such as FeCl₃ are formed which fortunately have boiling points that are different from that of SiHCl₃. This allows a technique called fractional distillation to be used, in which we heat up the mixture of SiHCl₃ and the impurity chlorides, and condense the vapors in different distillation towers held at appropriate temperature. We can thereby separate pure SiHCl₃ from the impurities. SiHCl₃ is then converted to highly pure EGS by reaction with H₂

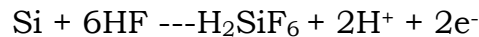
2.4 STRUCTURE:

Silica has a three-dimensional network structure. In silica, silicon is sp³-hybridized and is thus linked to four oxygen atoms and each oxygen atom is linked to two silicon atoms forming a three-dimensional giant molecule as shown in figure. This three-dimensional network structure

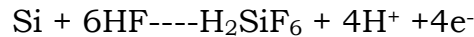
imparts stability to SiO₂ crystal and hence a large amount of energy is required to break the crystal lattice. As a result, SiO₂ is a hard solid with high melting point.

2.5 FORMATION OF POROUS SILICON

The exact dissolution chemistries of Si are still in question. And different mechanisms have been proposed. However, it is generally accepted that holes are required for both electro polishing and pores formation. During pore formation two hydrogen atoms evolve for every Si atoms dissolved. The hydrogen evolution diminishes approaching the electro polishing regime and disappears during electro polishing. Current efficiencies are about two electrons per dissolved Si atom during pore formation. And about four electrons in the electro polishing regime. The global anodic semi reactions can be written during pore formation as



And during electro polishing as



The final and stable product for Si in HF is in any case H₂SiF₆ or some of its ionized forms. This means that during pore formation only two of the four available Si electrons participate in an interfacial charge transfer, while the remaining two undergo corrosive hydrogen liberation. In contrast, during electro polishing all four Si electrons are electrochemically active.

Lehmann and Gosele have proposed a dissolution mechanism which is so far the most accepted (Fig.1.6) It is based on a surface bound oxidization scheme, with hole capture, and subsequent electron injection, which leads to the divalent.

According to Fig.2.1 the Si hydride bonds passivate the Si surface unless a hole is available. This hypothesis is also supported by the experimental observation that hydrogen gas continues to evolve from the porous layer after the release of the applied potential for a considerable time. In addition, various spectroscopic techniques have confirmed the presence of Si-H surface bonds during PS formation.

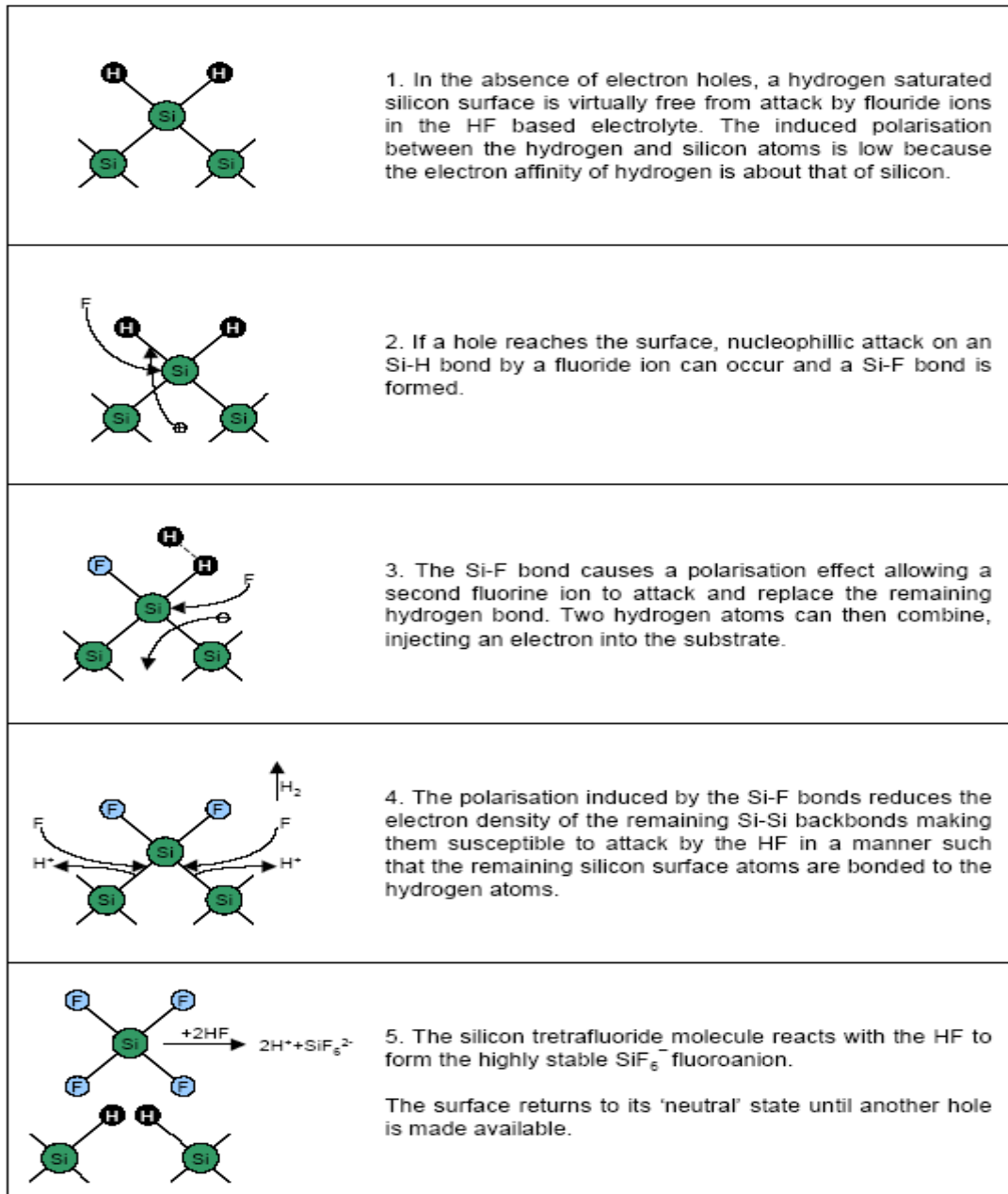


FIG:2.1 MACHANISAM OF FORMING PS

2.6 CONDUCTING POLYMER

The main conducting conjugated poly (p-phenylene), polyaniline, and poly (p-phenylenevinylene). These are important in view of scientific as well as industrial research. Conducting polymers are this class of material. They are basically classified by the conjugate nature of their bonding, the alternate singles and doubles bonding. The conducting polymers can be induced to transfer electrons to other materials such as Buckminster fullerene. It is observed that these conducting polymers have important electronic and optical properties like semiconductors or metals and advantage of mechanical properties and processing over the conventional materials.

2.7 SEMICONDUCTING POLYMERS

The discovery of conducting polymers has led to much interest in their application as microelectronic devices. Their advantage over conventional materials such as silicon and germanium is due to their cost effectiveness and simpler processing. Polymers, which are the constituents of familiar plastic materials and synthetic fibers, are large organic molecules built out of smaller ones linked together in a small chain. Generally, polymers are insulators. To make these substances conductive, the polymers are doped and the chain then becomes electrically unstable. Applying a voltage causes the electrons to flow across the length of the polymer. The majority of the semi conducting polymers has electrical conductivity in the range from 10^{-12} to 10^2 Ohm/cm (4). Semi conducting polymers have attracted much attention from fundamental and technological point of view. Most of these polymers have been used as bulk or thick films, resulting in the restriction of studies on their fundamental processes and their applications. Several synthetic methods of preparation of polymers like

polypyrrole, polyaniline and polythiophene have been developed. These methods usually produce black or brown powder, which is used for technological applications. These applications include sensor electrodes, positive electrodes in rechargeable batteries, corrosion protection, electro catalysis, antistatic coatings, electromagnetic shielding, electro chromic displays, gas separation and sensors.

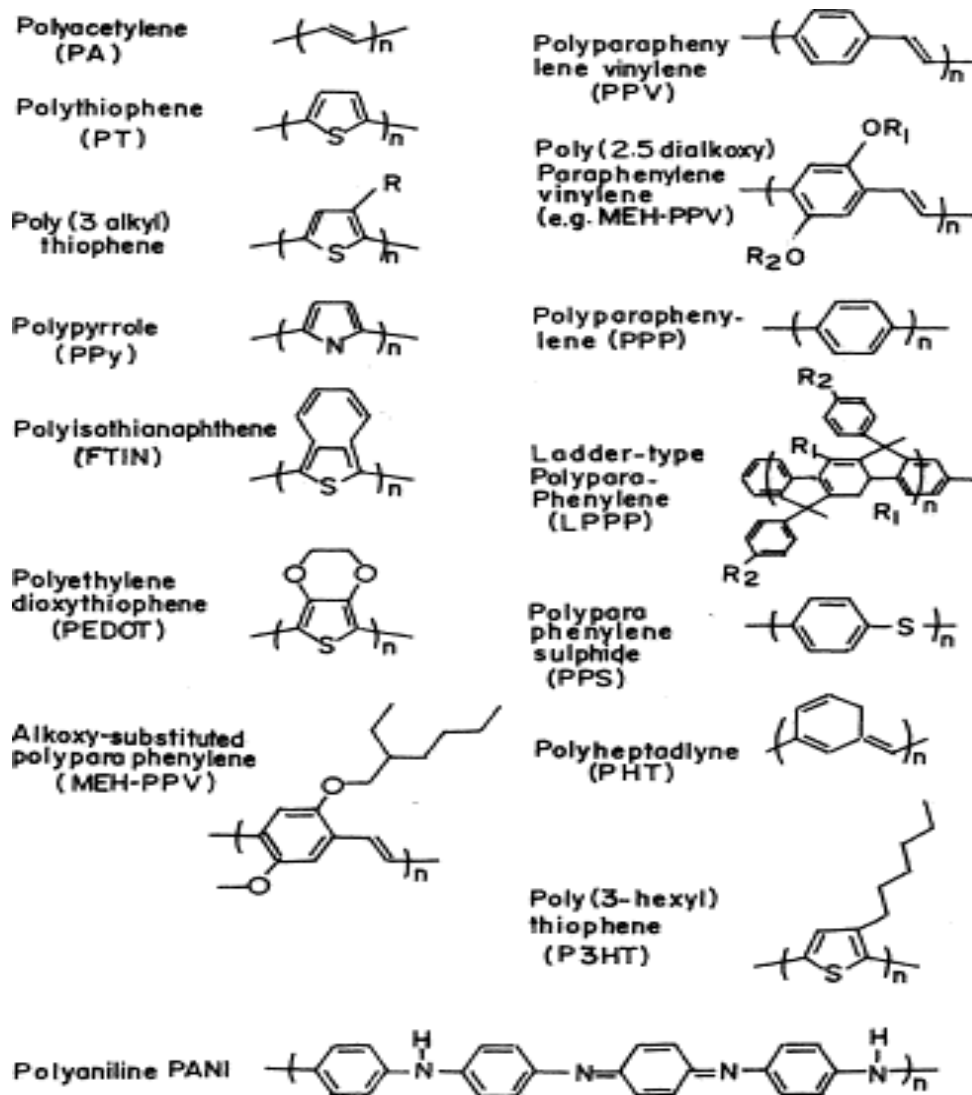


Fig.2.2 different conducting polymers

2.8 ADVANTAGES OF SEMICONDUCTORS CONJUGATED MOLECULES

1. Easy deposition, e.g. with spin coating or ink jet printing like process
2. Handling under ambient conditions possible-nitrogen atmosphere is preferable though
3. Relatively cheap large scale production
4. Electronic tunability (will be discussed in the section below)
5. High absorption coefficients in comparison to inorganic semiconductors
6. Polymers can be mixed easily when they dissolve in the same solvent, or can be
7. Separated in phases equally simple if they use incompatible solvents.
8. Many mechanical and chemical characteristics (e.g., solubility and strain, cross

Linking properties) can be fine tuned by adding and removing side groups

2.9 DOPING OF CONJUGATED POLYMERS

Polymeric photovoltaic present the tantalizing possibility of producing coatings that function sunlight harvesting paints on roofs or even as an integral part of fabrics to produce electricity from sunlight. MacDiarmid, Shirakawa, and Heeger (Nobel Prize winner in Chemistry, 2000) brought the unique properties of conjugated polymers to the fore in 1977 when they discovered that chemical doping level, a conductivity anywhere between that of the non-doped (insulating or semi conducting) and that of the fully doped (highly conducting) form of polymer can be easily obtained as shown in Fig. Conducting blends of a (doped) conducting polymer with a conventional polymer (insulator whose conductivity can be adjusted by varying the relative proportions of each

polymer, can be made. This permits the optimization of the best properties of each type of polymer. FIG from poly material

2.10 STUDY ON POLYPYRROLE

Polypyrrole is known since 1916. However, its semi conducting properties were first investigated by McNeill. PPY was first electrochemically synthesized as a black deposit in aqueous sulphuric acid medium anodically by Dall'Olio and has a conductivity of 8 Scm^{-1} .

Electrochemically synthesized film of polypyrrole has good mechanical strength. The electrolyte can be used for film synthesis are LiClO_4 , tetraethylammonium tetrafluoroborate (Et_4NBF_4), P-toluenesulphonate (PTS), HCl, etc, Electrode should be chosen carefully so that they are not oxidized during the electrochemical oxidation, The film is deposited on anode. The metals such as aluminum, indium, iron and silver are unsuitable for the polymerization of polypyrrole since they oxidized before polymerization occurs. Metal proposed as anode are chromium, gold, nickel, palladium, Platinum and titanium. However, the most suitable electrode proposed for the polymerization of pyrrole are platinum, gold, and glass coated with a conductive indium-tin oxide (ITO) and on PS also.

Growth of film depends on the nature of anion (electrolyte), solvent, monomer concentration, pH, temperature, the potential of electro polymerization and the amount of charge passed during polymerization. Morphological features of polypyrrole film vary between globular, cylindrical, fibrous and a non-uniform, amorphous surface features depends upon the nature of synthesis. The oxidation potential of polypyrrole is lower than the monomer pyrrole, thus the polymer is simultaneously oxidized during polymerization and hence counter ions

from electrolyte are incorporated into growing polymer in order to maintain electrical neutrality. Lower oxidation potential favors 2,5-bonded polymer on an anode surface. The polymerization of pyrrole can be effected by the presence of electrolytes under aqueous or non-aqueous condition. However, with oxidizing like NO_3^- and ClO_4^- yield a polymer having other than 2,5 linkage having a carbonyl and hydroxyl group. The conjugational length depends on the synthesis condition

In polymerization, the initial oxidation step produces a radical cation, which can either react with another radical cation to produce a dimer or undergo electrophilic attack on a neutral monomer. The electro polymerization reaction occurs only when the applied potential is sufficient to oxidize the monomer. The charge consumed during polymer formation has a linear time dependence and independent of pyrrole concentration. The dimer, trimer, and thus the polymer, polypyrrole are all more readily oxidized than the pyrrole monomer. And thus the polymer is neutral due to presence of anions, which are incorporated during the electro polymerization process. When PPY is reduced the conducting polymer backbone becomes neutral and the neutral and the overall polymer acquires a net negative charge. In order to maintain overall electrical neutrality either cations must be incorporated from surrounding solution or the anions previously incorporated must be expelled. When the PPY is subsequently re-oxidized, cations previously incorporated are expelled or anions present in the surrounding solution are incorporated. By cycling between its oxidized and reduced forms it is possible, therefore, to force the conduction polymer to act as both a cation and anion exchange material.

2.11 DIFFERENT METHODS FOR PREPARATION OF SEMICONDUCTING POLYMER FILMS

Technological development of semi conducting polymer is possible only when thin to thick films can be synthesized and characterized exhaustively. It is known that conducting polymer films have large surface to volume ratio, which consequently used to synthesize various conducting polymer films have been described below.

Vacuum deposition

1. Langmuir-Blodgett (LB) film deposition
2. Spin coating
3. Dip coating
4. Electrochemical polymerization
5. Sol-Gel Method
6. Physical method
7. Sputtering
8. Chemical method

2.11.1 VACUUM DEPOSITION

Vacuum deposition is a relatively a simple process that makes use of a chamber, a power supply elements capable of heating a material to a temperature at a required pressure. A vacuum pump system is capable of reducing the pressure sufficiently to allow the evaporation of the coating material and fix it in its position. It has now become possible to reduce thin layer deposits of semi conducting polymer by vacuum deposition techniques. Semi conducting polymer films formed by this technique are molecularly oriented and are parallel to the substrate (37).

Many organic materials can be evaporated by heating in vacuum, and can be formed into thin films by condensing the vapor on

substrates. This vacuum deposition technique has the advantage of depositing a film of thickness in nanometer range in the clean environment of high vacuum. Although the vacuum deposition is widely used for film preparation of inorganic materials in industrial scale, it has sparsely been applied for organic materials except for academic purpose, since the solution-based methods are considered to have higher throughput and cost performance. On the other hand, recent advancement of organic light emitting diode (LED's) was made possible by constructing multi-layered structures using vacuum deposition method. It indicates that the physical vapor deposition might be an indispensable technique for the development of future organic devices. It is therefore, industrially, as well as academically, important to pursue a new technology for depositing functional and high quality organic thin films.

2.11.2 LANGMUIR – BLODGETT (LB) FILM DEPOSITION

Langmuir-Blodgett technique has been applied for preparing organic thin films in which functional parts are arranged in ordered states (28,29). The feasibility of locating functional parts at the molecular level along with the control of the thickness of resultant films are the novel features of this technique. This technique includes two steps such as, the formation of stable monolayer films at air-water interface and subsequent transfer of the film onto a solid substrate.

A typical film forming molecule consists of hydrophilic part and hydrophobic part. The former usually, contains the functional moiety of the films of any alkyl chain. These built up monolayer assemblies on the substrates are now referred to as Langmuir-Blodgett films whereas the floating monolayer is termed as Langmuir monolayer. The hydrophilicity and hydrophobicity of the molecules play important roles in each step suggesting that the modification of hydrophilic part of the molecule

should result in films with different structures and functions even if functional moieties are in isolated form. Although the LB technique has proven to yield consistently near perfect long range ordering of monolayer and multiplayer (a30,31) of species that self-assemble at the liquid surface , it is cumbersome , time consuming and the required apparatus comes at great cost and maintenance .

2.11.3 SPIN COATING

Spin coating usually develops a radial variation of thickness (32). Spin coating is mostly used for depositing layers of photo resist as part of the patterning process in integrated circuit fabrication. Solution is poured onto the substrate surface, which is then spun to expel excess fluid and create a uniform thickness i.e. a relatively viscous polymer solution is placed onto the glass substrate to be coated at a fixed angular speed in range 500-4000 rpm. The polymer solution flows readily outwards to form a thin solution layer that subsequently Sets as the solvent evaporates. The uniformity of the layer depends on number of factors including the initial acceleration of the substrate and the rate of solvent evaporation. Both of which can be easily controlled.

2.11.4 DIP COATING

Dip coating a substrate with organic polymers may increase the efficiency of light-emitting diodes and computer displays while reducing costs and environmental hazards. Dip coating is a very simple process that binds a plastic solution to a substrate. Dip coating consists of three steps. In the first step, a coating is obtained by direct immersion of the substrate into the polymer solution. In the second step, removed substrate from solution and allowed excess coating material to drain into a collection tank and finally, dried or cured the substrate in the third

step. Dip coating is an easier, faster, and less expensive alternative to spin coating. However, it cannot achieve the high level of uniformity and the extremely thin layers that spin coating is capable of surface Cleaning and pretreatment are normally required to obtain a high quality.

2.11.5 ELECTROCHEMICAL POLYMERIZATION

Electrochemical polymerization is regarded as a simple and novel technique for the preparation of a desired conducting polymer film. Galvanostatic, potentiodynamic or cyclic voltametry techniques have been used for this purpose respectively. The films are prepared by stoichiometric polymerization of monomer in the presence of a desired electrolyte in a cell consisting of working, counter and reference electrodes, respectively. The heterocyclic compounds such as, polythiophene, polycarbazole, polyfuran, polypyrrole copolymer of pyrrole and polyaniline etc. are synthesized by this technique (33,34). In the electrochemical synthesis, the electro – polymerization is accompanied by simultaneous oxidation. The first step involves the oxidation of monomer to its radical cat- ion. Since electron transfer reaction is faster than the bulk solution and the second step involves the coupling of two radical cat ions to produce a dihydrodimer dication, which leads to dimer after loss of two protons and rearomatization (35,36).

2.11.6 SOL-GEL METHOD

This is the method in which transition of a system from a liquid sol (colloidal suspension of minute solid particles in liquid) to a viscous gel in which the suspended particles are organized in a loose but definite three-dimensional arrangement . The thin film gel is dried (this process can be repeated several times to achieve the required film thickness) and finally sintered.

2.11.7 PHYSICAL METHOD

This type of depositions takes place because of a physical reaction. In this process, the material (to be deposited) is physically moved on to the substrate. In other words, there is no chemical reaction, which forms the material on the substrate.

2.11.8 SPUTTERING

In sputter deposition, called sputtering, particles vaporized from a surface (sputter target) by the physical sputtering process. Physical sputtering is a non-thermal vaporization process. Surface atoms are physically ejected from the target materials when the accelerated ions (ion gun) impact with force and collected on a substrate. Sputter deposition is performed between the pressure 5-15 m Torr under vacuum or low – pressure gas (<5 m Torr) where the sputtered particles do not suffer gas – phase collisions in the space between the target and the substrate. This technique involves the generation of plasma and the directed acceleration of ions extracted from the plasma to a target material. The accelerated ions impact the target the target with such force that material is ejected from the target and collected on a substrate. In sputtering the sample is generally held 75 to 100 mm from the target. Sputtering is generally used to deposit metals, dielectrics, and semiconductors on flat substrates that are essentially two – dimensional.

2.11.9 CHEMICAL METHOD

In chemical method the deposition of conducting films takes place because of a chemical reaction. This process exploits the creation of solid materials directly from chemical reactions in gas and /or liquid compositions or with the substrate material. The solid material is usually not the only product formed by the reaction Byproducts can include gases, liquids and even other solids.

2.12 PREPARATION OF PANI, PPY & CO-POLYMER FILMS

The PANI films were prepared electro-chemically in potentiostatic mode at a potential of 0.8 Volts by 0.1 M HCl using a three electrode system(Potentiostat/ Galvanostat – 273A from Princeton Applied Research). Indium-tin-oxide (ITO) coated glass plates were used as working electrodes, and a platinum foil and Ag/ AgCl were used as the counter electrode and reference electrode respectively. The area used for the deposition of film was about 1 cm². The PANI films thus obtained were found to have electrical conductivity in the range of 10⁻¹ S/cm. The films were thoroughly washed with phosphate buffer prior to use. A set-up similar to the one used for fabrication of PANI films was adopted for preparation of PPY films. The films were deposited on ITO glass plate at a constant voltage of 0.8 Volts using a solution comprising pyrrole (15 µL) and Poly(Vinyl sulfonic acid) (30 µL). The co-polymer film was prepared by successive plating of poly-aniline and poly-pyrrole using the set-up and solutions as mentioned above.

CHAPTER 3

EXPERIMENTAL

3.1 INTRODUCCION

Semiconductor nanocrystals can be described as a state of matter intermediate between molecule and bulk crystalline. Their small size and high optical activity make them a very interesting material for study in disciplines ranging from optoelectronics (integrating optical and electronic signals on single substrates)(1,2). The development of efficient devices for detection of toxic gases and microorganism is an important challenge in sensor development area. The selection of proper configuration and material to act as selective interface to mediator between the outside environment and the sensor is crucial. The recent development of semi conducting materials, with every imaginable combination of physical and chemical characteristics for fabrication of sensors has lead to the fabrication of efficient gas sensors. The diversity of properties of these materials in various configuration enables them provide a wide range of applications in sensor technology (3). The sensors show excellent sensitivity in the thin film form. Porosity increases its thermal stability.

The nanocrystalline thin films are prepared by Electrochemical method; hence rely upon a dry technology. Platinum metal deposited on the material in the 10^{-6} mm Hg vacuum adjusting the time of deposition controlled the thickness of the films. The sensors were fabricated from thin films prepared on substrates (4). Characterization is an important step of identification of material in terms of its structure and functioning of a device wherein the material of interest is utilized. Various chemical, physical and physico-chemical techniques have been used for the characterization of conducting materials. Chemical characterization consists of elemental analysis and determination of oxidation states . Physical characterization involves electrical conductivity measurement, PL, FTIR, SEM ,X-ray diffraction, I-V characteristic techniques.

Semiconducting material have been shown to have applications in fabrication of sensing device, Schottky diodes have been fabricated using PS

as p-type semiconductor and various metals as ohmic and rectifying contacts. Current (I)-voltage (V) and capacitance ©-voltage (V) measurements on these devices have been performed to determine toxic gases and microorganism in the air in PPM levels. Keeping these points in mind, we have used Electrochemical deposition for the synthesis of various semiconducting PS films. These semiconducting polymers have been characterized by a number of techniques and have been used for their applications in fabrication of sensing device.

3.2 MATERIALS

Silicon wafer, Hydro fluoric acid (49%), Ethanol, hydrogen peroxide, Platinum, Aluminum, distil water, copper, methanol, water-vapors.

3.3 OTHER MATERIALS

Silver pest, Gold pest, Aluminum, NaOH, KOH,

3.4 SYNTHESIS OF SEMICONDUCTING POROUS NANOCRYSTALLINE SILICON

The promotion of Si from being the key materials for microelectronics to an interesting material for photonic applications is a consequence of the possibility to reduce its dimensionality by a cheap and easy technique. In fact, electrochemical etching of Si under controlled conditions leads to the formation of nanocrystalline Si where quantum confinement of photo excited carrier's yields to a band gap opening and an increased radiative transition rate. Efficient light emission is the product. The resulting material is named porous silicon (PS) due to its morphology composed by a disordered web of pores entering into Si. Its structure is like a sponge where quantum effects play a fundamental role, i.e. PS could be viewed as a quantum sponge, and as a sponge it can be permeated by a variety of

chemicals and its enormous internal surface rules its properties. These features (being a quantum system and a sponge) are keys both to the success and to the failure of PS. In fact, many possible applications exploit the quantum confinement (e.g. in light emitting diodes) or the high reactivity of its surface (e.g. sensor applications) but to promote PS to real and commercial devices one has to master its quantum sponge nature. The disordered distribution of nanocrystal sizes, interconnectivities, and surface compositions hampers a real engineering of PS properties. Its enormous and active inner surface causes time and ambient dependent properties, aging effects and uncontrolled deterioration of device performances. It is an interesting piece of scientific work in the understanding of the properties of this material and the mastering of some of its properties to obtain devices which work in a predictable way. Here we try to present an overview of this work.

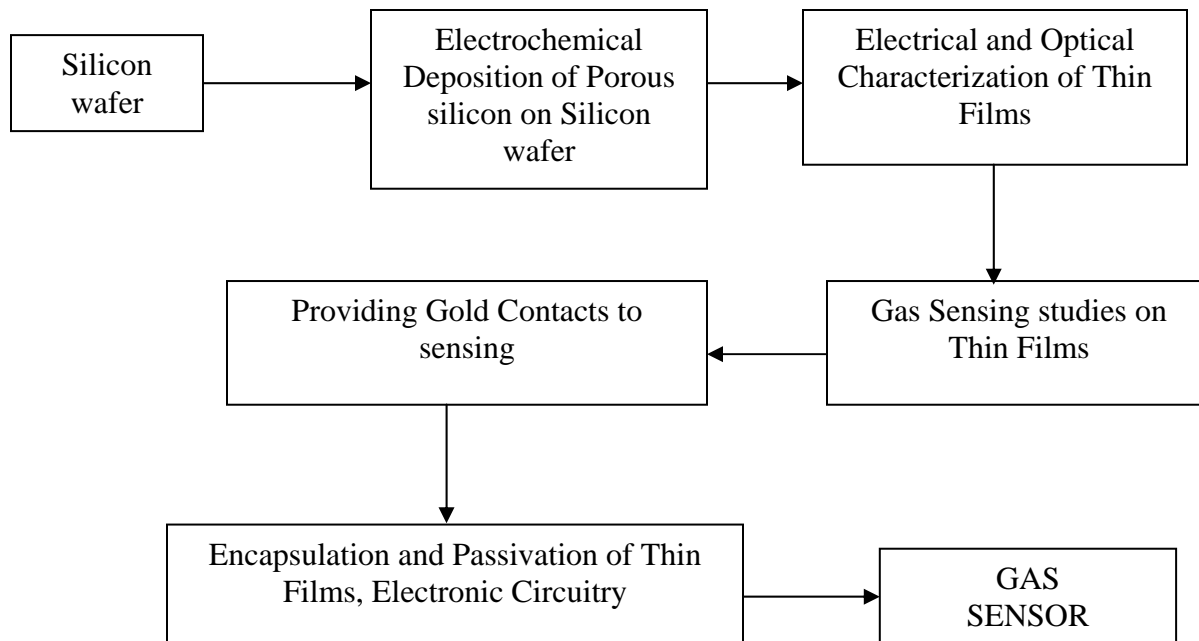


Fig:3.1 - Block diagram for preparation of gas sensor

3.5 ELECTROCHEMICAL FORMATION

Boron doped p type Si wafers of (100) orientation; 8-10 ohm cm resistivity and 400 cm thickness were used for preparing PS. The wafers

were polished in 40% NaOH for 2 minutes. These wafers were textured using 2% NaOH at 85°C for 30 minutes. For forming the back contact, Ag-Al paste was screen printed on the wafer and dried at 250°C. The wafer was then heated to 750°C for 2 min in an IR furnace. PS was formed by the standard anodization process using Si as the anode and Pt as the counter electrode in an acid resistant container. The anodization was carried out at 20 to 50 mA cm⁻² for 30 mins, in two different electrolytes. The first is a mixture of HF and C₂H₅OH (1:1 by volume), which is almost universally used [1] and would be abbreviated as electrolyte A. The second is a mixture of HF and H₂O₂ (1:1 by volume), which was extensively used by Nafeh and co-workers [12] and would be abbreviated as electrolyte B. After the anodization, the films were washed in deionized water and ethanol and dried in nitrogen. The samples were subjected to continuous agitation in an ultrasonic cleaner to evaluate the speed with which the sample is destroyed. The weight of the sample is continuously monitored.

Electrolyte Usually, HF is sold in an aqueous solution with up to 49% of HF. Thus. The first attempts to form PS were performed using only HF diluted in deionized and ultra-pure water. Due to the hydrophobic character of the clean Si surface, absolute ethanol is usually added to the aqueous solution to increase the wet ability of the PS surface, In fact, ethanoic solution infiltrate the pores, while purely aqueous HF solution do not. This is very important for the lateral homogeneity and the uniformity of the PS layer in depth. In addition, during the reaction there is hydrogen evolution. Bubbles form and stick on the Si surface in pure aqueous solutions, whereas they are promptly removed if ethanol (or some other surfactant) is present. For the same reason, a careful design of the anodization cell is necessary in order to promote hydrogen bubble removal. Moreover, it has been found that lateral in homogeneity and surface roughness can be reduced, increasing

electrolyte viscosity, either by diminishing the temperature or introducing glycerol to the composition of the HF solution.

Potential. The dissolution is obtained either controlling the anodic current or the potential. Generally, it is preferable to work with constant current, because it allows a better control of porosity, thickness and reproducibility of the PS layer.

Cells. The simplest electrochemical cell is a Teflon beaker. The Si wafer acts as the anode and the cathode is generally made of platinum, or other HF-resistant and conductive material. The cell body is usually made of a highly acid resistant polymer such as Teflon. Using this cell PS is formed all over the wafer surface exposed to HF, including the cleaved edges. The advantages of this cell geometry are the simplicity of equipment and the ability to anodize silicon-on-insulator structures. The drawback is the inhomogeneity in porosity and thickness of PS layers, mainly due to a potential drop. In fact, there is a difference in potential between the top and the bottom. Leading to different values of local current density.

The second type of anodization cell is shown in Fig a. In this cell, the Si wafer is placed on a metal disk and sealed through an O-ring, so that only the front side of the sample is used, a high dose implantation on the back surface of the wafer is required to improve the electrical contact between the wafer and the metal disk. This step is crucial to get later homogeneity in the PS layer. This cell is the most widely used because it leads to uniform PS layers, allows an easy control of both porosity and thickness, and it is suitable for front side illumination of the sample during the attack.

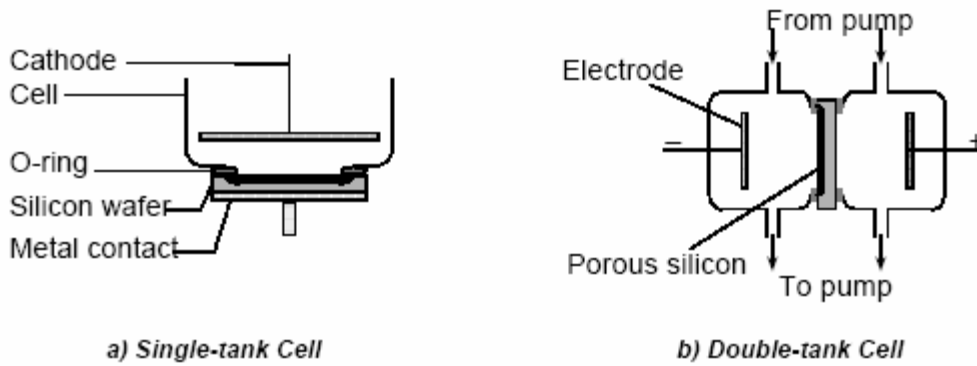


Fig.3.2 Electrochemical anodization a) Single tank Cell b) Double tank Cell

The third type of anodization cell is double tank geometry with an electrolytic backside contact. This cell (Fig b.) consists of two half-cell in which Pt electrodes are immersed and the Si wafer is used to separate the two half-cell. HF solution, circulated by chemical pumps to remove the gas bubbles and avoid the decrease in the local concentration of HF, is used both to etch the front side and as a back contact. A better uniformity is obtained using symmetrical and large Pt plates as the cathode and the anode. The current flows from one electrode to the other through the Si wafer. While stirring of the solution has shown no major effects on the quality of the PS layer, the HF circulation during the etch helps to achieve a good depth uniformity and it is also preferable for security reasons. The use of closed loop pumps to circulate the electrolyte is possible also for the other geometries. The backside of the Si wafer acts as a secondary cathode where proton reduction takes place leading to hydrogen evolution. While the front side of the wafer acts as a secondary anode, where PS is formed. Since the backside contact is made, electrolytically no metalization is required, but a high dose implantation is still necessary for high resistive wafers. The uniformity of the layers obtained under these conditions is comparable to that with a single-tank cell. Most of the problems encountered with the solid back contact in highly resistive samples are greatly reduced. If illumination is required, the material used in the cell should be Plexiglas, which is

transparent and HF resistant (up to 15% HF) With this cell. Both front and backside illumination is possible.

A recent suggestion is to use a lateral geometry for PS formation. An electrical contact is deposited on the very same surface on which PS will be formed. In this way, the PS formation does not proceed in depth but in lateral direction. Very flat PS\Si interfaces are so realized.

<u>Electrochemical method</u>		
Wafer used	:-	P-type Si wafer
Electrolyte	:-	(A)HF: Ethanol or(B)HF:H ₂ O ₂ in [1:1] ratio
Potential		
Current density	:-	10, 20, 35 mA/cm ²
Current	:-	11.3, 22.61, 39.5 mA
Voltage	:-	3 Volts
Time	:-	30 mints

Table:3.1 - Specification for Electrochemical method

3.6 PORE FORMATION

What it is generally accepted that pore initiation occurs at surface defects or irregularities different models have been proposed to explain pore formation in PS. Some basic requirements have to be fulfilled for electrochemical pore formation to occur.

4. Holes must be supplied by bulk Si, and be available at the surface.
5. While the pore walls have to be passivated, the pore tips have to be active in the dissolution reaction. Consequently, a surface which is depleted of holes is passivated to electrochemical attack. Which means that
 - (i) The electrochemical etching is self-limiting and
 - (ii) Holes depletion occurs only when every hole that reaches the surface reacts immediately. Mass transfer in the electrolyte does not limit the chemical reaction.
6. The current density should be lower than the electro polishing critical value. For current densities above such a value, the reaction is under ionic mass transfer control, which leads to a surface charged of holes and to a smoothing of Si surface (electro polishing). The behavior at high current densities turns out to be useful to produce PS freestanding layers. Raising the current density above the critical value at the end of the anodization process results in a detachment of the PS film from the Si substrate

3.7 EFFECT OF ANODIZATION CONDITIONS

All the Properties of PS, such as porosity, thickness, pore diameter and microstructure, depend on anodization conditions. These conditions include HF concentration, current density, wafer type and

resistivity, anodization duration, illumination (n-type mainly), temperature, ambient humidity and drying conditions

An increase of. Yields a	Porosity	Etching rate	Critical current
HF concentration	Decreases	Decreases	Increases
Current density	Increases	Increases	-
Anodization time	Increases	Almost constant	-
Temperature	-	-	Increases
Wafer doping (p-type)	Decreases	Increases	Increases
Wafer doping (n-type)	Increases	Increases	-

Table:3.2 - Effects of Electrochemical method and conditions

Porosity is defined as the fraction of void within the PS layer and can be easily determined by weight measurement. The wafer is weighted before anodization (m_1), just after anodization (m_2). And after a rapid dissolution of the whole porous layer in a NaOH or KOH solution (m_3). The porosity is given by the following equation;

$$P (\%) = (m_1 - m_2) / (m_1 - m_3).$$

Guessing the Si density p , one can also get the PS layer thickness d

$$d = m_1 - m_3 / pS$$

Where S is the etched surface.

For p-type doped substrates, and for a given HF concentration the porosity increases with increasing current density. For fixed current density, the porosity decreases with HF concentration. With fixed HF concentration and current density, the porosity increases with thickness and porosity gradients in depth occur.

This happens because of the extra chemical dissolution of PS layer in HF.

The thicker the layer, the longer the anodization time, and the longer the residence of Si in the HF reaches solutions.

Porous thickness measurement

$$\begin{aligned} \text{Porous thickness (t)} &= m_2 - m_3 / A * \rho \\ &= \text{Weight of the porous silicon without} \\ &\text{pour} / \text{Area} * \text{density} \end{aligned}$$

$$\begin{aligned} \text{Area of the porous silicon} &= \pi r^2 \\ &= \pi (1.2/2)^2 \text{ cm}^2 \\ &= 3.14 * 0.36 = 1.13 \text{ cm}^2 \end{aligned}$$

Density of silicon = 2.23gm/cm³

Layer thickness of the samples was estimated using the relation:

$$H = m_1 - m_3 / A\rho$$

Where, A is the cross sectional area of the sample and ρ is the density of silicon. Uniformity factor, measure of pore branching has also been estimated with different formation parameters using the relation:

$$U = j / j_{ps}P$$

Where, j is the formation current density, P is the measured porosity and j_{ps} is the critical current density for lateral electro polishing.

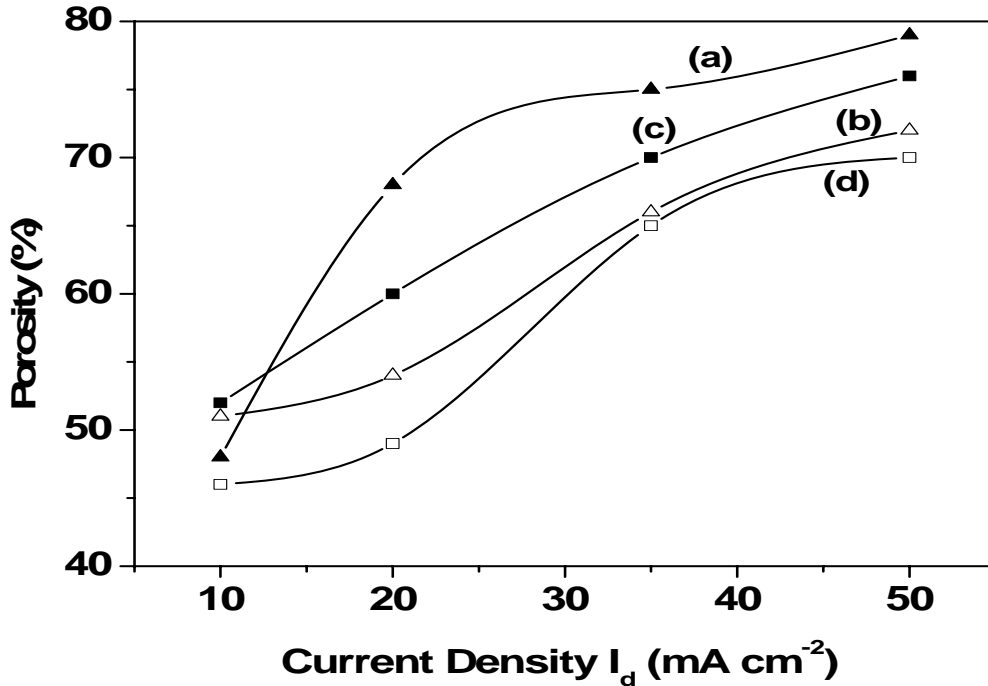


Fig.3.3 Porosity of PS as a function of current density (I_d); (a) Textured substrate, Electrolyte B; (b) Polished substrate, Electrolyte B; (c) Textured substrate, Electrolyte A; (d) Polished substrate, Electrolyte A.

3.8 DIFFERENT TYPES OF PS

In the low current density region, where PS forms, some considerations apply, A surface region depleted in mobile carriers is formed at the Si/electrolyte interface. This region is highly resistive (comparable to intrinsic Si). The thickness of the depleted region depends on the doping density. It is several nm thick for lightly n-type doped Si. It is thin for highly n- or p-type doped Si, and it does not exist for lightly to moderately p-type doped Si. The size of the pores is related both to the depletion layer width and to

the mechanism of charge transfer. In highly doped substrates charge transfer is dominated by tunneling of the carriers, and the pore size reflects the width of the depletion region, being typically around 10nm. In lightly n-type doped Si anodized in the dark, generation of carriers occurs at breakdown. The pore dimensions are about 10-100 nm (mesopores), regardless of doping density. Under illumination the pore size is dependent on doping density and anodization conditions, with diameters in the range 0.1-20mm(macro pores). A whole depletion is expected in any case if the dimensions of the nanocrystals are about few nanometers, independent of the substrate type and doping. In this size region Quantum confinement is effective and the Si band gap is increased. A hole needs to overcome an energy barrier to enter this region. This highly improbable. The quantum confinement is responsible for pore diameters below 2 nm, denoted as micropores. Micro pores can be found on every type of PS samples, but only in moderately and lightly p-type doped substrates pure micro PS exists. Both mechanisms coexist during PS formation, resulting in a super position of micro and meso (or macro) structures, whose average size and distribution depends on substrate and anodization condition.

Pore with (nm)	Type of pores
<2	Micro
2-50	Meso
>50	Macro

Table:3.3 - types of PS according to porosity

3.9 FORMATION OF POROUS SILICON

The exact dissolution chemistries of Si are still in question. And different mechanisms have been proposed. However, it is generally accepted that holes are required for both electro polishing and pores formation. During pore formation two hydrogen atoms evolve for every Si atoms dissolved. The hydrogen evolution diminishes approaching the electro polishing regime and disappears during electro polishing. Current efficiencies are about two electrons per dissolved Si atom during pore formation. And about four electrons in the electro polishing regime. The global anodic semireactions can be written during pore formation as



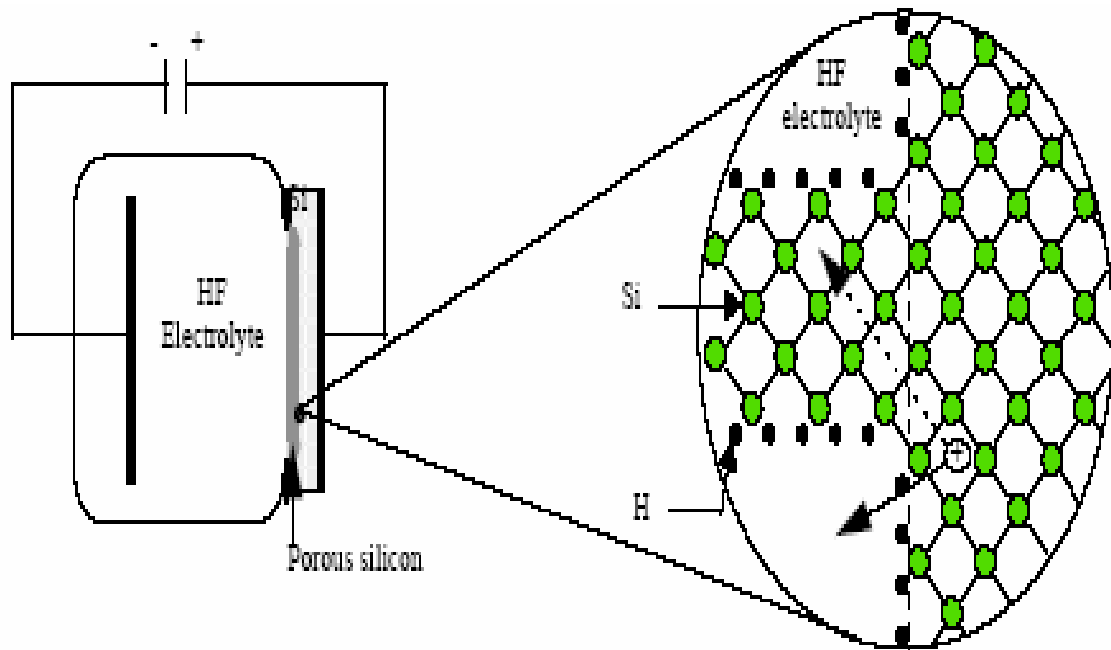
And during electro polishing as



The final and stable product for Si in HF is in any case H_2SiF_6 or some of its ionized forms. This means that during pore formation only two of the four available Si electrons participate in an interfacial charge transfer, while the remaining two undergo corrosive hydrogen liberation. In contrast, during electro polishing all four Si electrons are electrochemically active.

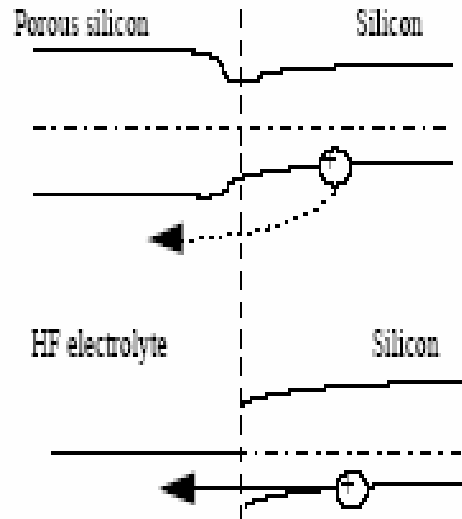
Lehmann and Gosele have proposed a dissolution mechanism which is so far the most accepted (Fig.3.4) It is based on a surface bound oxidization scheme, with hole capture, and subsequent electron

injection, which leads to the divalent Si oxidization state.



Top left - schematic diagram for the formation of porous silicon

Top right - silicon branch isolated by two pores. Two possible ways for the hole to cross the silicon - porous silicon interface are shown (broken and dotted arrow).



Bottom - band diagram of the silicon - porous silicon interface and the two different energy barriers for the hole penetrating into the wall (broken arrow) or into the electrolyte (solid arrow)

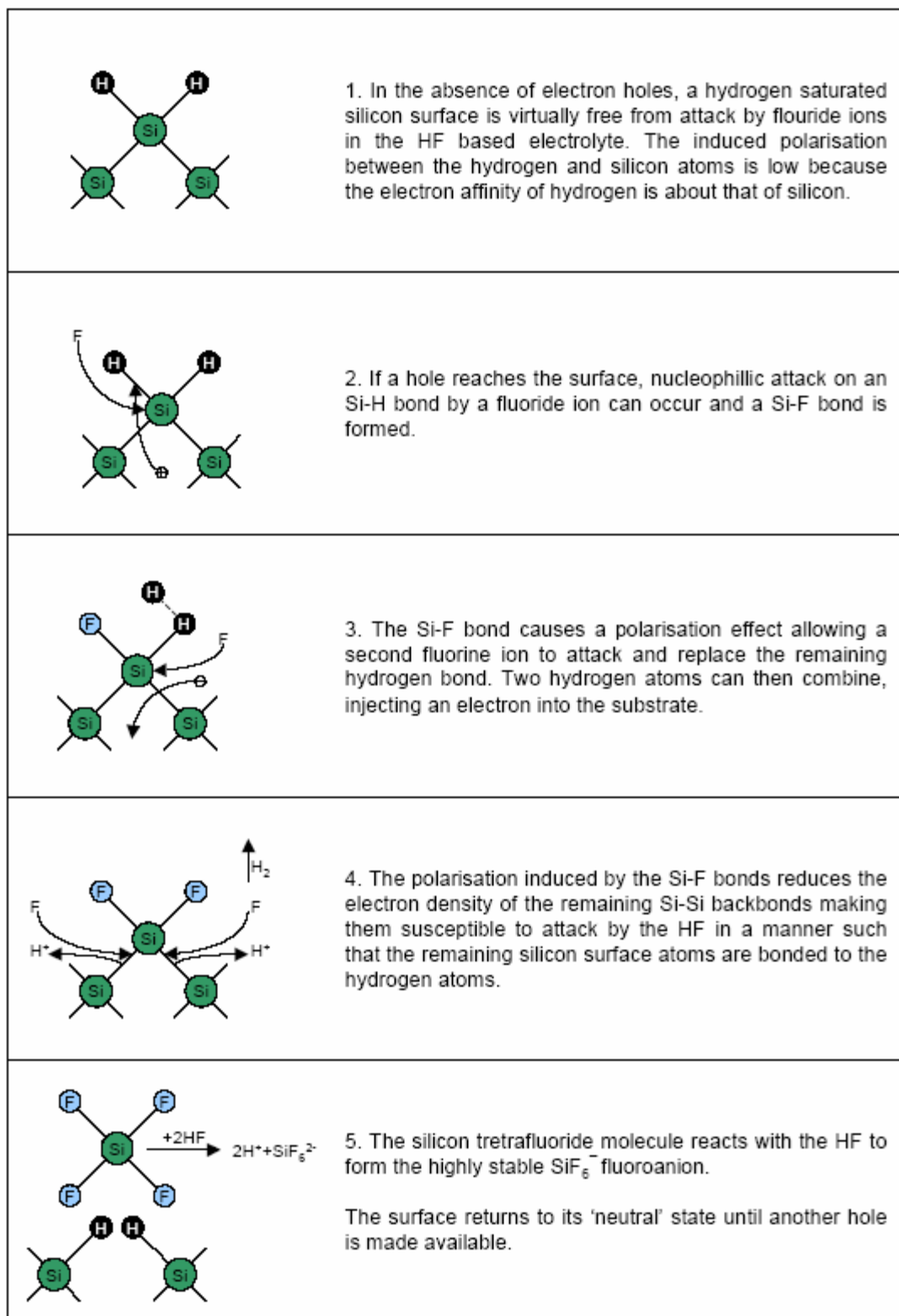


FIG: 3.4 -MACHANISAM OF FORMING PS

According to Fig.3.4 the Si hydride bonds passivate the Si surface unless a hole is available. This hypothesis is also supported by the experimental observation that hydrogen gas continues to evolve from the porous layer after the release of the applied potential for a considerable time. In addition, various spectroscopic techniques have confirmed the presence of Si-H surface bonds during PS formation.

3.10 DRYING OF THE SAMPLES

The drying of PS layers, especially those of high porosities, is a crucial step. After the formation of a highly porous or thick PS layer, when the electrolyte evaporates out of the pores, a cracking of the layer is systematically observed. The origin of the cracking is the large capillary stress associated with the evaporation from the pores. After the anodization, the films were washed in deionized water and ethanol and dried in nitrogen. The samples were subjected to continuous agitation in an ultrasonic cleaner to evaluate the speed with which the sample is destroyed. The weight of the sample is continuously monitored.

3.11 POLYMER COATED POROUS SILICON

On Porous Silicon Polymer coated by Electrochemical method by Princeton Applied Research Potentiostat /Galvanostat model 273A this set up for supply accurate constant voltage by taking parameters as shown in table.

Porous Silicon taken as working material, counter material (C) as Pt and Reference material (R) as Ag/AgCl and electrolyte taken as mixer of H₂O, PVS (polyvinyl Sulphonic acid) solution, 0.1 M Pyrrol. Electrochemical reaction carried at 0.95 V for 300 Sec. By that polypyrrol was coated on Porous Silicon.

<u>Electrochemical method</u>		
Wafer used	:-	P-type Si wafer
Electrolyte	:-	H₂O+PVS+0.1M Pyrrol
Counter material C	:-	Pt
Working material W	:-	Si
Reference material R	:-	Ag/AgCl
Voltage	:-	0.95 Volts
Time	:-	300Sec

Table.3.4 Electrochemical method for coating PPY on Porous Silicon

CHAPTER 4

ELECTRICAL & OPTICAL CHARACTERIZATION

ELECTRICAL AND OPTICAL CHARACTERIZATION OF THIN FILMS

4.1 MORPHOLOGY OF THE RESULTING LAYERS

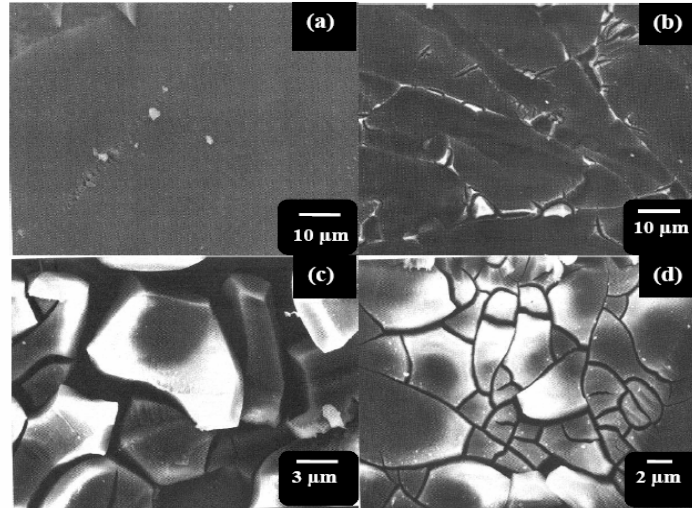


Fig.4.1 Scanning electron micrographs of porous silicon prepared on polished substrates at different current densities (I_d); (a) $I_d = 10 \text{ mA cm}^{-2}$, Electrolyte A; (b) $I_d = 10 \text{ mA cm}^{-2}$, Electrolyte B; (c) $I_d = 35 \text{ mA cm}^{-2}$, Electrolyte A; (d) $I_d = 35 \text{ mA cm}^{-2}$, Electrolyte B.

The scanning electron microscope (SEM) has become one of the most widely utilized instruments for materials characterization. It is an incredible tool. Conventional light microscopes use a series of glass lenses to bend light waves and create a magnified image, while the SEM creates the magnified images by using electrons instead of light waves. The SEM shows very detailed 3-dimensional images at much higher magnifications than is possible with a light microscope. SEM has been widely used for the visualization of organic surfaces, especially in the study of surface morphology, domains, pinhole defects and patterns of the porous silicon formed on textured and polished Si-substrates at different densities the magnification is 1000, which is small and does not show the silicon nanowires. Fig.4.1 show the surface of porous silicon

formed on silicon at current densities of 10mA cm^{-2} and 35mA cm^{-2} respectively. A plain featureless surface morphology is observed at 10 mA cm^{-2} while a highly cracked surface morphology is obtained at 35mAcm^{-2} . The surface is also not flat and the cracking has resulted in the release of stress and an undulating surface indicated by changes in SEM contrast. The higher current density results in increased porosity and the inability of the silicon nanowires to withstand the stress leads to cracking. Similar observations on the fragility of thick and highly porous films had been noted earlier¹. On further raising the current density, 35mAcm^{-2} , more pronounced cracking and delaminating is observed Fig.4.1 shows the surface morphology of porous silicon formed on substrates at 35mAcm^{-2} , the surface morphology consists of randomly sized and spaced pyramids homogeneously distributed on the surface. However, the pyramids appear to be more sharply separated. There is however, no evidence of any fracture or cracks formation. The surface morphology for current densities is not different.

4.2 AFM image of pores

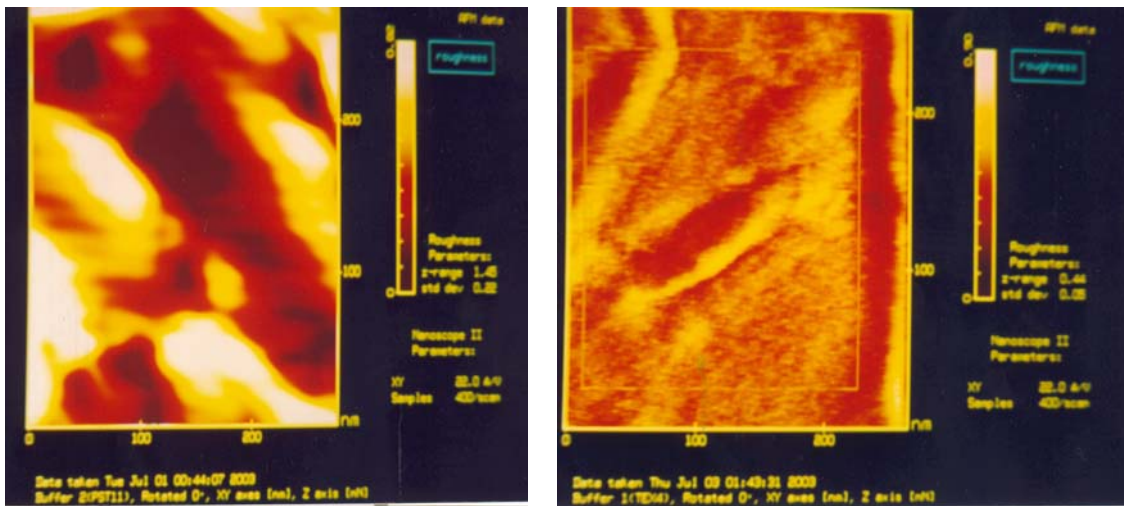


Fig.4.2 The AFM image of the textured porous silicon surface shows large (100 nm) size pores at some regions. This is not seen in textured silicon or in porous silicon formed on polished silicon substrates

The surface morphology of the porous silicon layer measured by AFM is given in Figure, which shows that the surface of the PS layer

consists of inhomogeneous and large number of irregularly shaped pores and voids distributed randomly over the entire surface. We have earlier shown that the electrochemical etching of Si surface shows excellent surface texture with significant variation in surface morphology of the PS can be expected across the surface as a function of etching time for different anodization currents and longer etching times lead to deeper and irregular features on the PS surface.

4.3 PHOTOLUMINESCENCE

The PL was measured using a home assembled system consisting of a two stage monochromator, a photomultiplier tube (PMT) with a lock-in amplifier for PL detection, and an Ar⁺ ion laser operating at 488 nm and 5 mW (corresponding to 0.125 W cm⁻²) for excitation in all the measurements. Decay of PL intensity has been used as a measure of the stability of the surface bond configurations [7]. For PL decay studies, the sample was continuously exposed to the laser radiation and PL measurements were

The presence of large number of unsaturated bonds on the surface of PS has a profound effect on the PL efficiency and stability. Changes in surface bonding of the exposed surface area cause a complex evolution of the luminescence intensity. As shown in figure 3, significant decay of the PL intensity is observed for PS film ($I_d = 20 \text{ mA cm}^{-2}$) formed on untextured silicon. However, for PS film formed on textured silicon at the same current density, no PL decay was observed. In our PS samples ($I_d = 20 \text{ mA cm}^{-2}$) prepared on untextured substrates, the PL band is at ~700-720 nm. No change in this value is observed by variation of the current density or by the use of textured silicon. Typical results are shown in as an inset in fig. 3. The above PL decay results are a direct evidence of association of stable surface bonds with stable textured PS surface.

According to Canham's [1] and subsequent works [32], an increase in current density or an increase in PS porosity always led to a blue shift of the PL spectra. However, in our study, the surprising difference is that there is no appreciable change in PL peak position with variation of the current density either for textured or untextured substrates. Another point of contention is that why the texturization of Si-substrates lowers the stress formation on PS films. As already mentioned earlier, that PS film formation depends on the crystallographic directions with growth rate more for $\langle 100 \rangle$ as compared to $\langle 111 \rangle$ [17], however its relation to stress has not been reported so far.

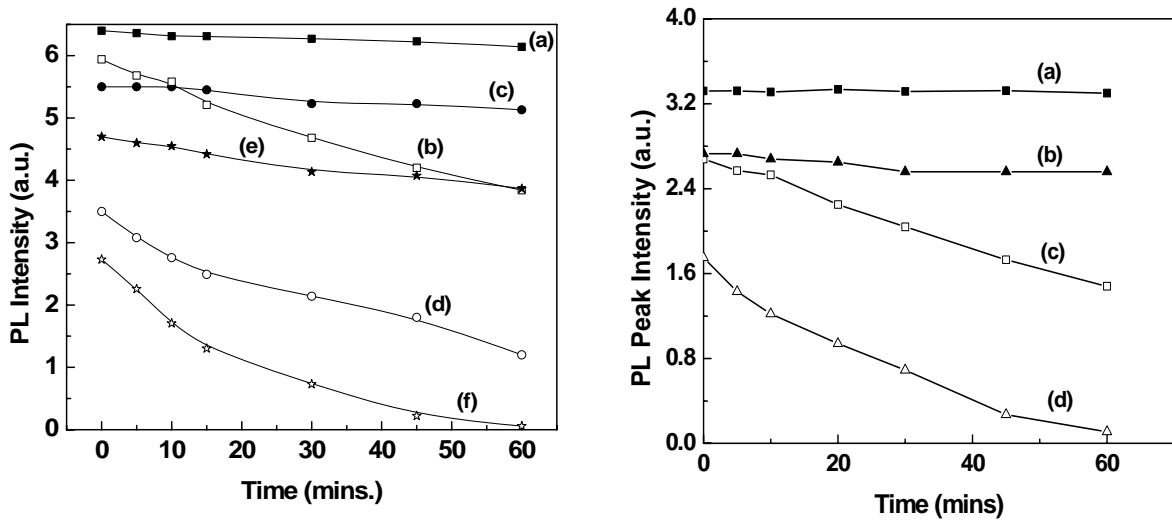


Fig.4.3 PL spectra of porous silicon samples prepared at different current densities (I_d) for (A) electrolyte A and (B) electrolyte B; (a) Textured substrate, $I_d = 20 \text{ mA cm}^{-2}$; (b) Polished substrate, $I_d = 20 \text{ mA cm}^{-2}$; (c) Textured substrate, $I_d = 35 \text{ mA cm}^{-2}$; (d) Polished substrate, $I_d = 35 \text{ mA cm}^{-2}$ (e) Textured substrate, $I_d = 50 \text{ mA cm}^{-2}$ and (f) Polished substrate, $I_d = 50 \text{ mA cm}^{-2}$.

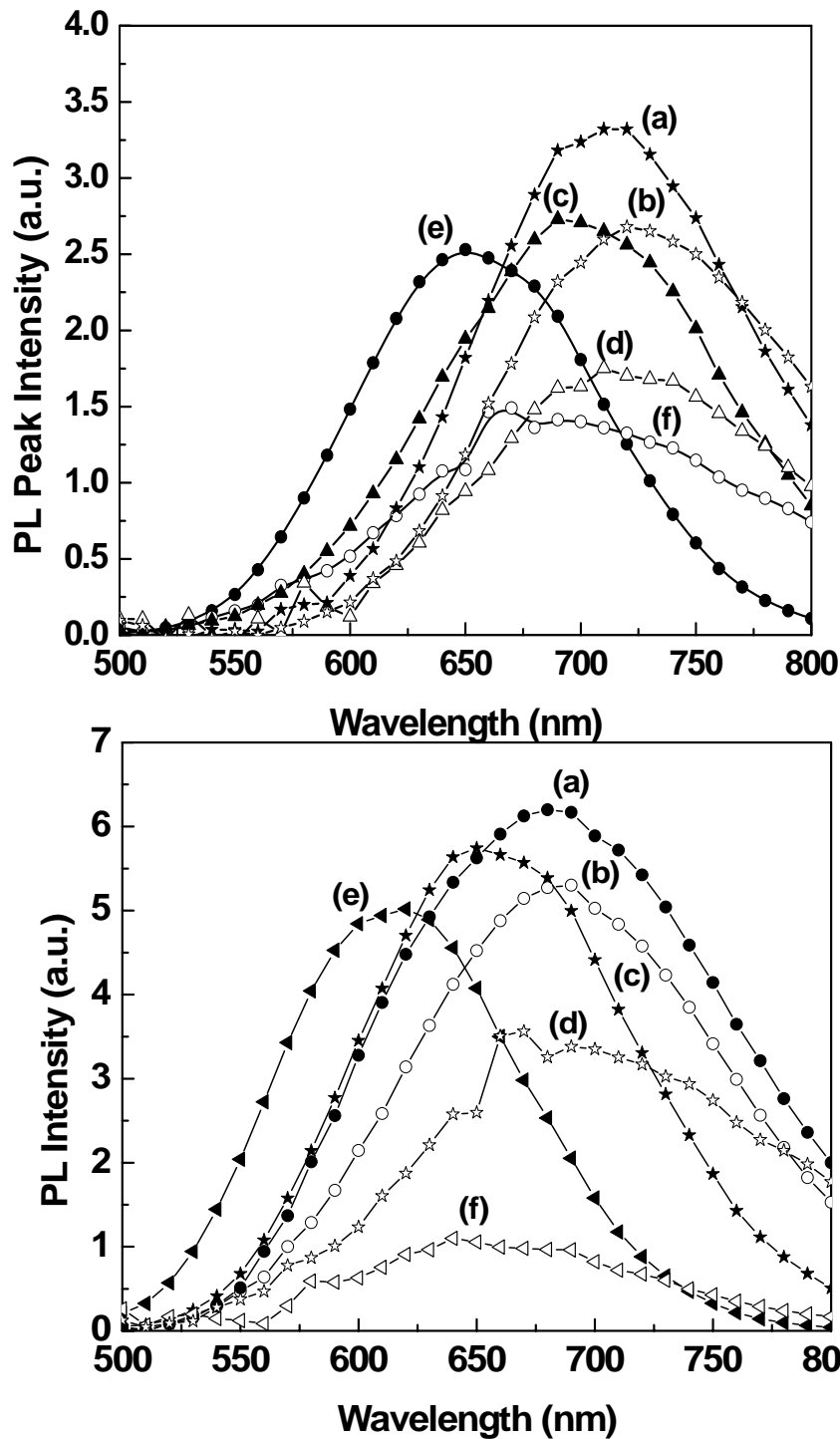


Fig.4.4 PL spectra of porous silicon samples prepared at different current densities (I_d) for (A) electrolyte A and (B) electrolyte B; (a) Textured substrate, $I_d = 20 \text{ mA cm}^{-2}$; (b) Polished substrate, $I_d = 20 \text{ mA cm}^{-2}$; (c) Textured substrate, $I_d = 35 \text{ mA cm}^{-2}$; (d) Polished substrate, $I_d = 35 \text{ mA cm}^{-2}$ (e) Textured substrate, $I_d = 50 \text{ mA cm}^{-2}$ and (f) Polished substrate, $I_d = 50 \text{ mA cm}^{-2}$.

The micropore formation on p-type silicon is not well documented and needs to be understood properly. There are different school of thoughts for macropore formation on p-type silicon viz: based on passivation effects where the absorption of organic molecules on the electrode is proposed to change locally the rate of silicon dissolution rather than space charge region effects usually observed for n-type silicon [33]; electrostatic considerations where the resistivity of the silicon electrode is higher than that of the electrolyte, then every perturbation on the interface is enhanced by accumulated field lines [34]. However, both models are found to be in contradiction with experimental observations. The main model, which has been widely accepted, has been that of Lehmann and Ronnebeck [35], which is based on the charge-transfer mechanism in a Schottky diode with a nonplanar interface. Here, the silicon electrode anodized in HF is under depletion in the regime of porous silicon formation and behaves therefore like a solid state Schottky-diode. However, the origin of stress in PS is still currently under debate. The proposed mechanisms for PL are (i) quantum size effects in silicon columns [1]; (ii) surface SiH_x [32]; (iii) amorphous Si [36]; (iv) siloxene [37]. However, there seems to be no complete experimental evidence, which can definitely point out particular relationship between stress and PL mechanism in PS.

Thus, in case of PS films formed on textured Si-substrates, there is uniformity in PS porosity where higher PS porosity leads to lowering of stress and stress gets released on the surface of PS owing to plastic deformation. However, in the case of PS formation on untextured substrates, the stress does not get released resulting in formation of cracks or fracture.

The SEM and PL decay results essentially conforms that PS films on textured substrates at an optimum I_d are stress-free and are superior in crystalline quality, mechanical strength and has long term usability.

The results indicate conclusively that textured silicon substrates results in the formation of porous silicon with lower fragility and superior stability. However, this is not so in the case of untextured silicon substrates, where mechanically weak, unstable and fractured PS films are obtained presumably due to higher stress. The exact reason behind the lowering of stress for PS formed on textured substrates is not known and needs further study. A detailed investigation is underway.

4.4 FTIR

The structural features of the interface formed between the metal – pcs on the PS were studied by FTIR measurement measured in the range wave number 400-4000cm⁻¹. it reveals that the surface is characterized by chemical species like Si-H, Si-O, O-Si-H and C=O etc. co-existing on the surface. The presence of hydrogen related species on the PS layer could provide to extent a surface passivation effect (21). The various stretching and bending bonds were identified corresponding to the Si-H or Si-O surface species, and is given in Table. A broad band

Surface Species	Peak Position	Mode
Si-H	2248	Stretching in O ₃ -Si-H
Si-H ₂	2136	Stretching in Si ₂ -H-Si-H
Si-O	1110	Stretching in O-Si-O and C-Si-O
C-H ₃	1437	Bending in H-Si-H
Si-O	1437	Stretching in O-Si-O
Si-O	827	Stretching in O-Si-O
Si-H	630	Bending in H-Si-H

Table.4.1 Peak Positions of Surface Species by FTIR method

At 2100 cm⁻¹ is due to the surface Si-H_x stretching mode; a strong peak at 2260 cm⁻¹

Corresponds to O-Si-H_x (22). The FTIR data of the oxidized PS layer surface that a simultaneous decrease of intensity of the Si-H₂ peaks and disappearance of the hydrogen and oxygen related bonds as a result of thermal oxidation (at temperature >800°C under oxygen ambient) have also been observed. A strong peak at 1100 cm⁻¹ due to the presence of Si-O or Si-O_x, stretching bonds were observed in the FTIR spectra for the oxidized PS layer. The partial thermal oxidation of the Ps layers on Si substrate has a significant effect on the surface morphology and the porosity of the PS surface (11). This shown that dangling bonds associated with the PS surface are saturated with rich oxygen terminated SiO₂ layer and desorption of the surface state mechanism upon thermal beating is responsible for the disappearance of the hydrogen – terminated Si-H or Si-H_x species (23,24). These result show that low porosity PS layers formed on Si substrate is a possible candidate as use as an effective AR coating for large area silicon solar cells due to excellent surface texture, reduced refractive index and reduced surface reflection losses if the PS layer of a optimum thickness satisfied the conditions required for minimum reflection losses.

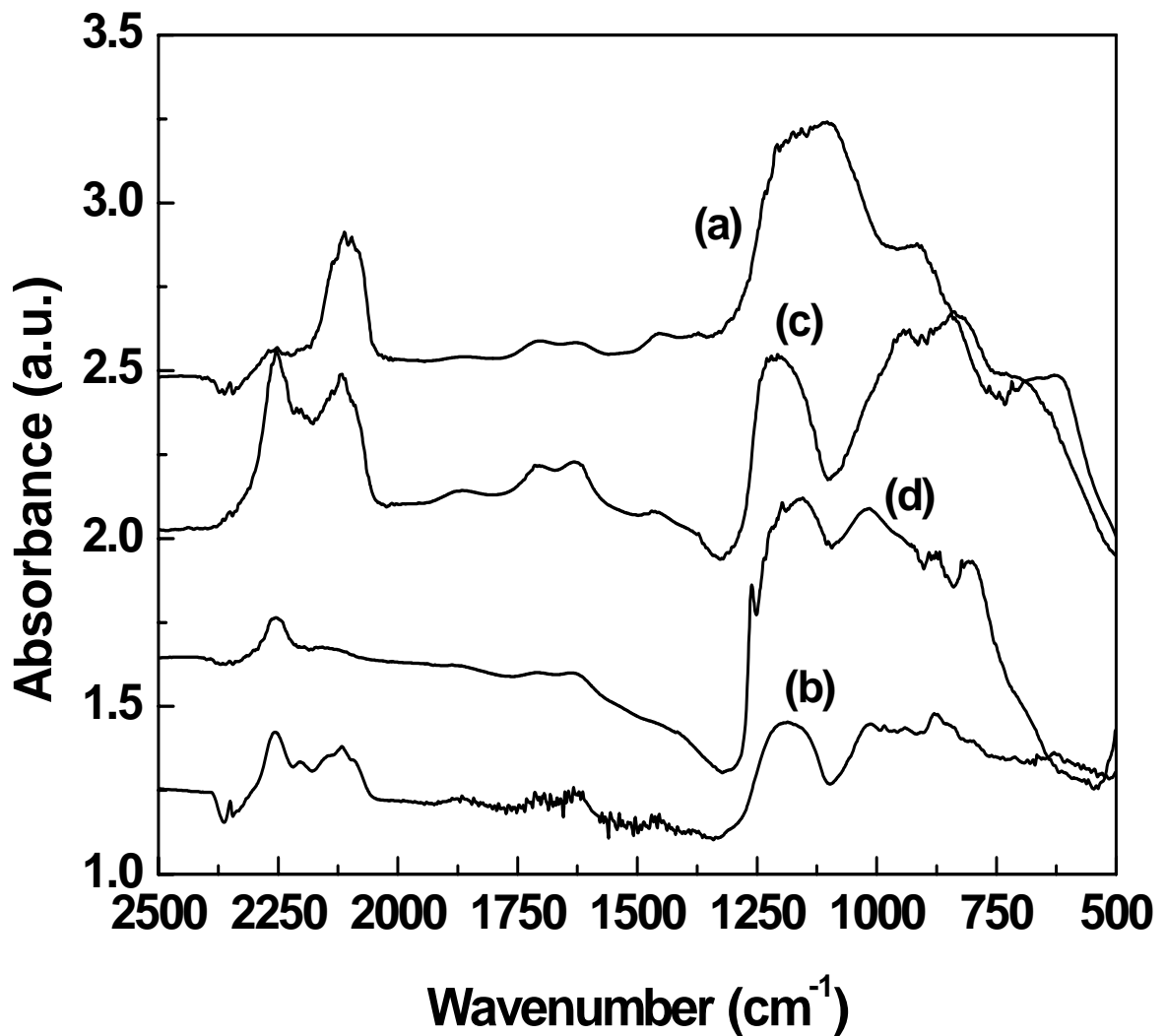


Fig:4.5 FTIR absorption spectra of porous silicon prepared at current density $I_d = 20 \text{ mA cm}^{-2}$; (a) Textured substrate, Electrolyte A; (b) Polished substrate, Electrolyte A; (c) Textured substrate, Electrolyte B; (d) Polished substrate, Electrolyte B.

4.5 SENSING MATERIALS OR CONTACTS FOR GAS SENSOR

1. Metals
2. Semi conducting oxides
3. Polymers

Pt, Al, In, Ni, Cu, gold related to metals. Conducting electrodes like I T O (indium tin oxide), P E O (phenylene vinyl oligomer) related to semi conducting oxides and poly pyrroline, polyaniline are related to polymers. These metals are coated over PS sample as a electrical sensor metals that means to calculate resistivity, sensitivity. These sensing metals coated over PS sample by vacuum pumping systems.

4.5.1 VACUUM PUMPING SYSTEMS:

The HINDHIVAC combined high vacuum pumping systems are used for our sensing material. These systems give an ultimate vacuum of 10⁻⁵ m.bar or better. In our case we are using Model VS-114. To achieve better ultimate vacuum the system the system should incorporate suitable traps like foreline trap, liquid nitrogen cold trap or chevron baffle as per the requirement. Our system is water-cooled type. They can be connected for creating vacuum in laboratory systems, lamp manufacturing units, T.V.tubes manufacturing, X-ray, distillation plants, and vacuum furnaces et

4.5.2 NICKEL COATING: -

1. Prepare the solution and test the PH level.

Water 50 cc

Nickel sulphate 1 gm

Ammonium fluoride 9gm

2. Ammonium solution to make the pH of the solution 7 to 8
3. Dip the PS (may be with Ag Al coating) for 10 to 20 min. until babbles stop
4. Dry
5. After the proper coating, resistance will be the order of few Ohms
6. with and without (+ve) Photoresist for masking
7. Wash it in acetone by that mask is removed and only Nickel coated area on PS remains.
8. Dry in oven for 20 min or 15min
9. Ag Al is pasted over sample
10. Heated at 700°C in a furnace to make good contact for 45 Seconds
11. Soldering

4.6 DEVICE FABRICATION

The above block diagram shows in (FIG) the flow of signal. The first block is the sensing part where a gas sensor is connected in series with a high value resistor and making a potential divider arrangement, The sensor is passive type sensor so it required a less volt supply and the flow of current is depending upon the variation of sensor resistance and hence the voltage appears on the out put terminal is proportional to the variation of resistance due to variation of gas.

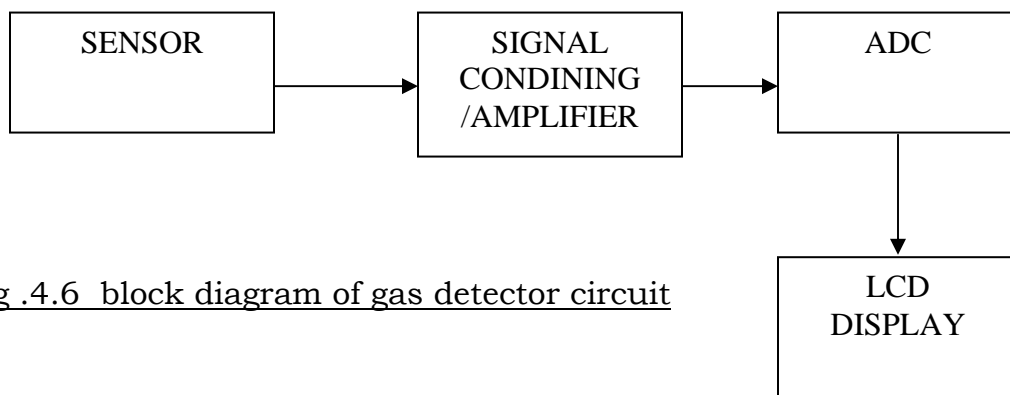


Fig .4.6 block diagram of gas detector circuit

Since this voltage is very low so it is fed in a high gain amplifier for amplification of the signal then it is faded to the ADC (analog to digital signal converter) where this analog signal is converted into digital signal and this digital signal is than displayed on the LCD display panel.

This circuit has a feature to use it for different types of toxic gases. The only change is required on this circuit is the sensor and calibration for the different gases because the variation of resistance of the sensing material is different for different gases.

47 ENERGY BAND DIAGRAM ANALYSIS

Porous silicon is a p-type semiconductor and the conduction in PS thin films is due to the hopping transport of polarons and bipolarons. The polarons and bipolarons become mobilized under the action of electric field in a sensor configuration. These charge carriers move intra –chain, inter-chain and through intercrystallites. The conduction in PS thin film accurse by crossing over of the charge carriers through the intercrystallites boundaries (FIG), which offer a charge barrier. This makes the Electrochemical deposited film to behave semiconducting.

When the thin films are exposed to gases like carbon monoxide, they result in a reduction of the barrier height at the intercrystallite grain boundary, thus lowering the intercrystallite barrier (FIG). This increases the current flow through the sensor. Hence, there is an increase in the current output from the sensor. The lowering of the barrier height is directly proportional to the amount of the gas absorbed by the thin film and hence the increase in the sensor output.

4.8 RESPONSE TIME ANALYSIS

Rise and decay of the current output of the PS thin film sensor for various concentrations of gas shows the sensitivity (current response) is directly proportional to concentration of gas, when the sensor is removed from the gas environment, the output decreases to a minimum value and the sensor recovers to original state in about 8seconds. The total response time is therefore of the order of 8-10 seconds. As the sensor is reusable, it is evident that there is no chemical reaction between PS film and the exposure species. Only a physical adsorption of gas on the vacuum deposited thin film takes place. This also is proven by the fact that the specificity and selectivity of the sensor is achieved by selectively doping the PS during sensor preparation. This sensor can be hooked up with necessary electronic to provide audio video alarm for continuous online monitoring.

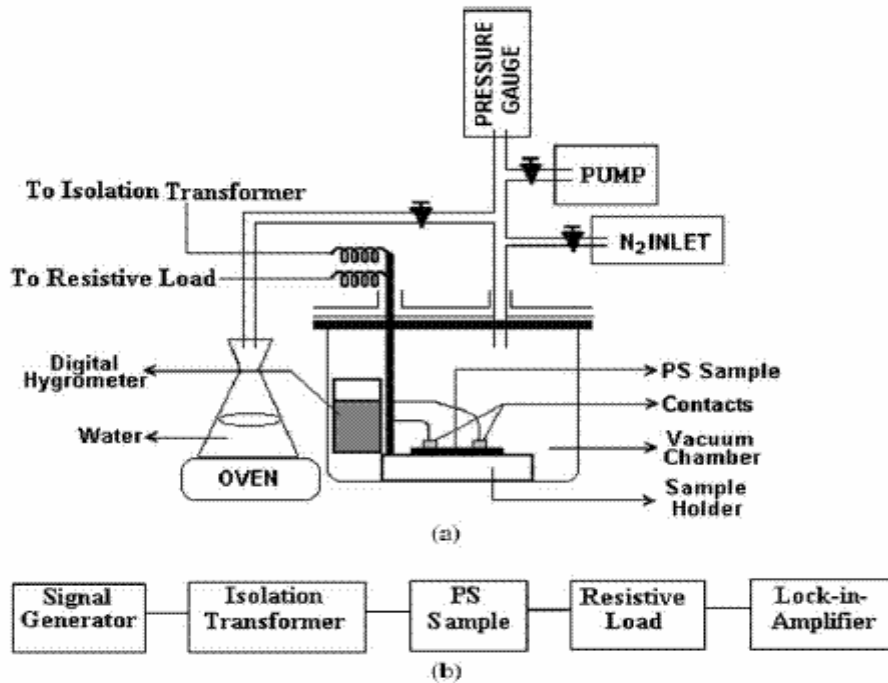


Fig.4.7 Total diagram of gas sensor.

After the formation of PS, samples were exposed to vapours of ethanol, methanol and humidity for different intervals of time and changes in electrical resistivity were monitored. The PL & FTIR of the PS sample before and after exposure to gases was also carried out. The detailed results are given in next chapter.

4.9 SPECIFICATION FOR GAS SENSOR

Specification	Gas
1.Doping	None
2.Detection principle	Amperometric
3.Operating Temperature	Room Temperature
4.Response Time	8-10 sec.
5.Minimum readable conc.	0.02 ppm
6.Specificity and selectivity	High
7.Sensitivity	Good
8.Power Requirements	<1mw
9.Sensor life	2-4 years
10.Accuracy	+5%
11.Output	Linear

Table 4.2 - specification for gas sensor

CHAPTER 5

RESULTS & DISCUSSION

RESULTS & DISCUSSION:

5.1 PHOTOLUMINESCENCE

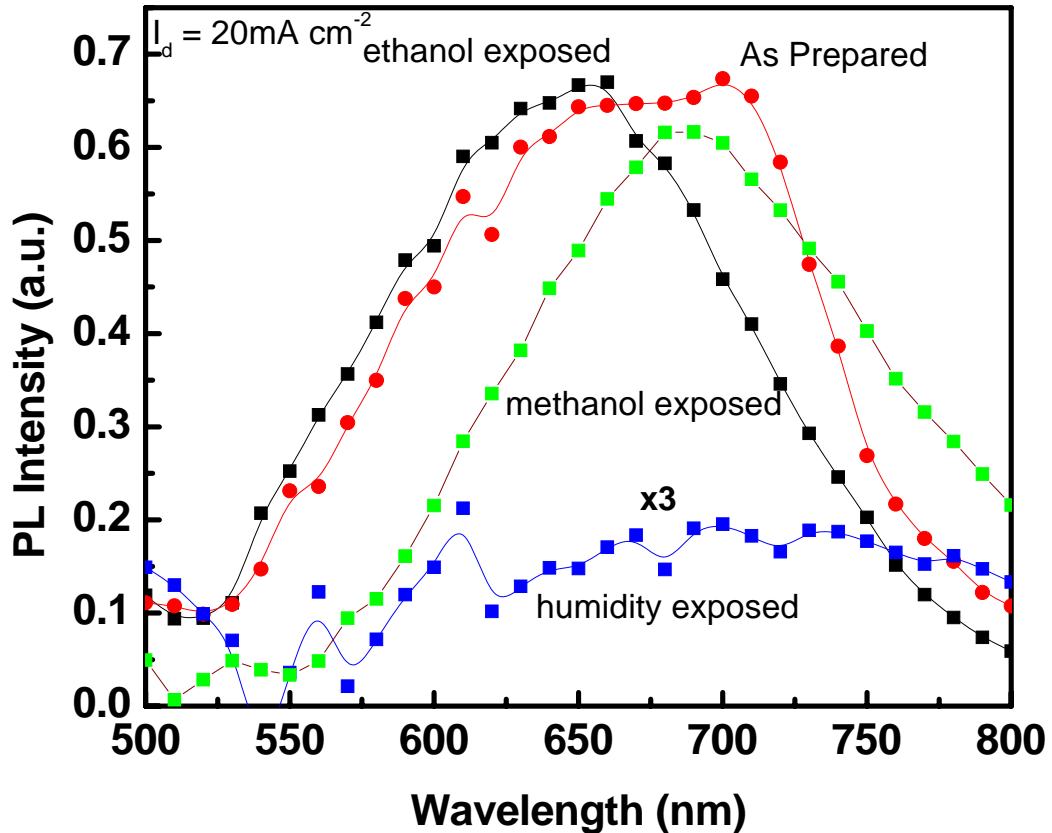


Fig.5.1 PL spectra of porous silicon sample exposed at different gases

For measuring the sensitivity to gases, the samples were placed in a test chamber and diluted ethanol, methanol and water-vapors using argon as the carrier gas were passed over them and corresponding changes in photoluminescence and electrical resistivity were monitored at different intervals of time. A blue-shift in PL peak position from 700 nm to 600 nm was observed for PS sample prepared at $I_d = 20 \text{ mA cm}^{-2}$ when exposed to ethanol vapors for 20 mins. However, the PL intensity remains the same upon exposure to ethanol. However, PS sample when

exposed to H₂O-vapours exhibits a drastic reduction in PL intensity and a relatively higher blue-shift in PL from 700 nm to 560 nm as compared to ethanol-exposed PS sample for the same time of exposure. The PS sample shows lower response towards methanol gas as evident from a marginal reduction in PL intensity and blue-shift in PL peak position from 700 nm to 690 nm respectively.

5.2 FTIR

The bonding features of the PS were studied by FTIR measurements in the range wave number 400-4000cm⁻¹. It reveals that the surface is characterized by chemical species. The PS sample was exposed to different gases and corresponding changes in bonding were observed by FTIR. Humidity exposed PS sample showed vast changes particularly in the Si-H stretching mode (~ 2100 cm⁻¹) and in Si-O related modes at 1050 cm⁻¹. An increment in Si-O mode with a concomitant decrease in Si-H mode was observed and it seemed that there is a change in surface passivation from hydride terminated to oxygen terminated. Similarly, with ethanol exposure of PS films, substantial changes in Si-H and Si-O modes were observed. Apart from this, Si-C modes were also evident at ~ 2400 cm⁻¹.

The improved gas sensing properties are attributed to the formation of highly porous vertical layers separating macroscopic domains of nanoporous silicon.

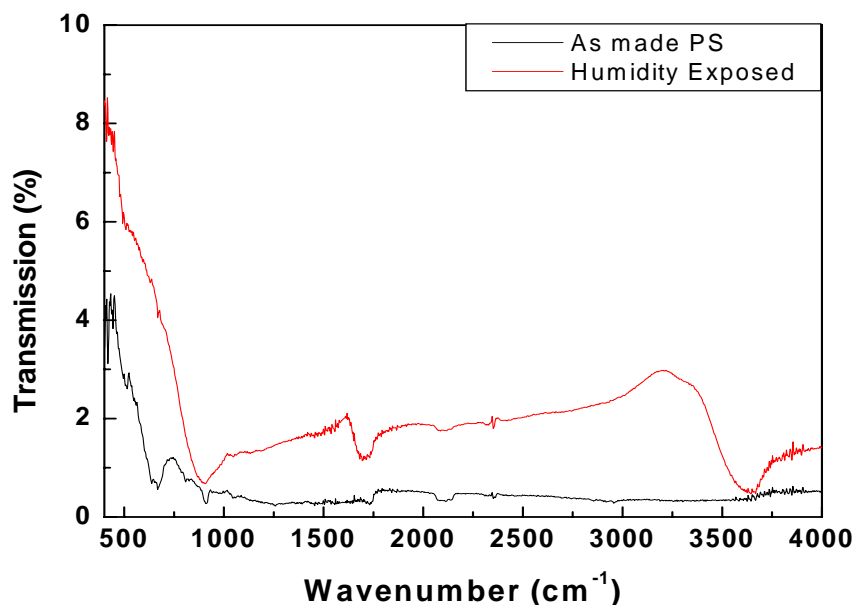
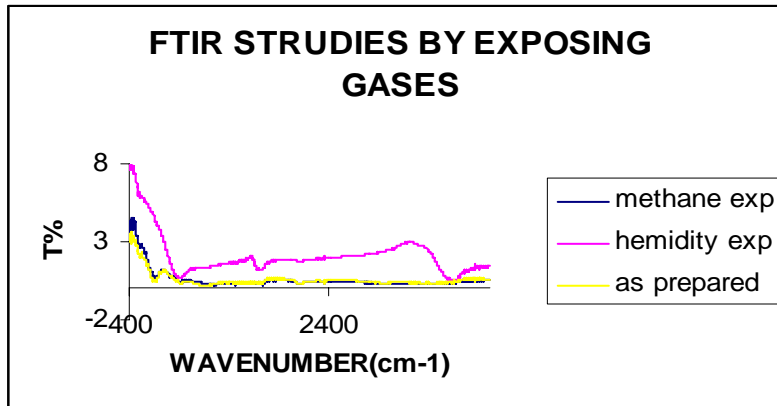


Fig.5.2 FTIR transmission spectra of porous silicon prepared at current density $I_d = 20 \text{ mA cm}^{-2}$; (a) Gas studies by exposing different gases (b) as made PS and Humidity Exposed.

5.3 Study of polymer coated Porous silicon

Polymer (PPY) was coated on porous silicon by Electrochemical method by this we where observed some improvement in peak intensity as observed by comparing by FTIR of as prepared PS. So that by coating conducting polymer we can get good resistivity and sensitivity. As shown in fig we observed changes at Si-oxygen and Si-hydrogen bond.

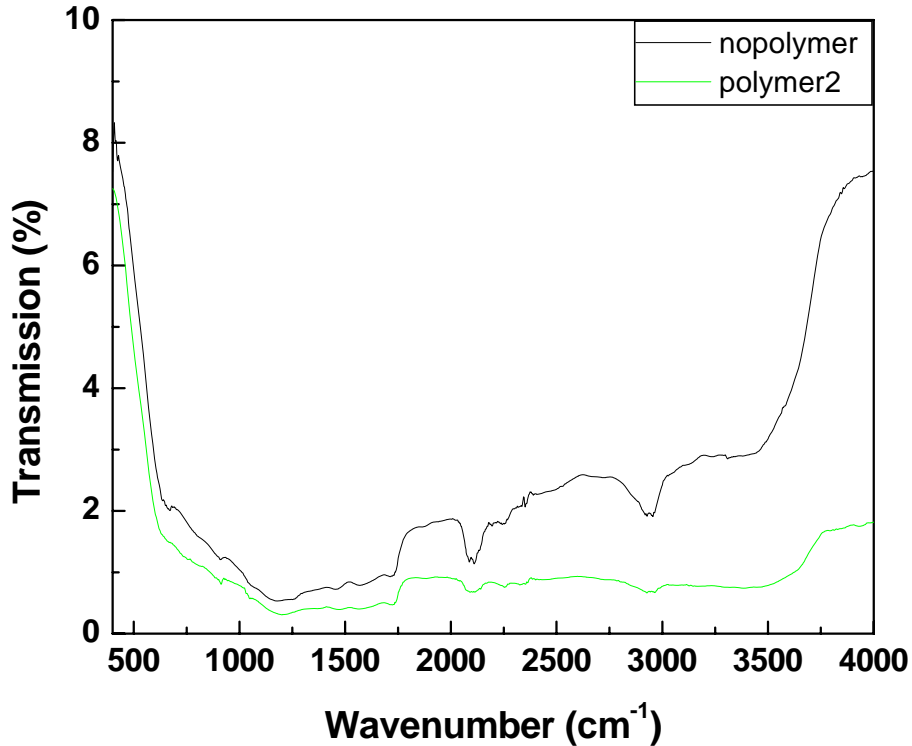


Fig.5.3 FTIR transmission spectra of porous silicon prepared at current density $I_d = 20 \text{ mA cm}^{-2}$; before coated and after coated with polymer

5.4 SENSITIVITY:

Sensitivity calculated by set up as shown in fig() by exposed with different gasses by heating or by Applying pressure on liquid by that liquid converted into gas

The sensitivity for detecting the presence of gas through resistivity measurement is defined as

$$S = \frac{R_0 - R_g}{R_0} * 100$$

Where $\Delta R = R_0 - R_g$ change in resistance before & after expose of a gas

R_0 = resistance before expose of gas

R_g = resistance after expose of gas

Resistivity of PS is correlated to the quantum confinement effect. Because of the high resistive surface with large surface states, which trap the carriers,

I_d (mA cm ⁻²)	Gas	Resistance (unexposed) R_0 (x 10 ⁶ ohm)		Resistance (exposed) R_g (x 10 ⁶ ohm)		Sensitivity ($\Delta R/R$) (%)	
		R_{par}	R_{perp}	R_{par}	R_{perp}	S_{par}	S_{perp}
10	Ethanol	0.3	8	0.035	1.8	88.3	77.5
20	Ethanol	18	0.92	1.2	0.18	93.3	80.4
35	Ethanol	0.5*10 ⁵	0.5*10 ⁵	0.112	0.5	99.9	99.9
10	Humidity	1.3	0.47	0.071	0.029	94.5	93.8
20	Humidity	16.5	1.07	0.131	0.077	99.2	92.8
35	Humidity	3*10 ⁵	3*10 ⁵	0.035	0.072	99.9	99.9
10	Methanol	0.4	8	0.3	4	25	50
20	Methanol	7.2	3.9	4.5	0.3	37.5	92.3
35	Methanol	6.3	1.03	4.1	0.16	35	84.4

Table.5.1 Calculating change of resistance and resistivity as prepared and after exposed.

PS sample prepared at $I_d = 20$ mA cm⁻² shows maximum sensitivity for both ethanol and humidity. For methanol-exposed sample ($I_d = 20$ & 35 mA cm⁻²), Sensitivity_{perp} is higher as compared to Sensitivity_{par}.

Sensitivity values in general increases with increase in current density particularly for ethanol and humidity.

Resistivity studies reveal that PS sample prepared at $I_d = 20 \text{ mA cm}^{-2}$ shows maximum and minimum sensitivity ($\Delta R/R$) values $\sim 90\%$ for both ethanol and humidity and $\sim 40\%$ for methanol gas respectively. With increase in current density, the response time in general decreases and the sensitivity value increases for PS samples upon exposure to ethanol and humidity in particular.

5.5 CONCLUSION

In this work, texturization of silicon surface has been demonstrated to be a simple and effective method for the formation of highly luminescent, thick films of porous silicon with reduced stress, improved stability and superior mechanical properties [5]. The present work is a systematic follow-up of that initial observation and its role in gas sensor applications has been envisaged. PS was formed by anodization process with boron doped (100) textured Si wafers (8-10 $\Omega \text{ cm}$, 400 μm thick) as the anode and Pt as the counter electrode in an acid resistant cell. PS films were made at current densities (I_d) between 10 to 35 mA/cm^2 range for 30 min. in HF-C₂H₅OH (1:1 by volume). For measuring the sensitivity to gases, the samples were placed in a test chamber and diluted ethanol, methanol and water-vapors using argon as the carrier gas were passed over them and corresponding changes in photoluminescence and electrical resistivity were monitored at different intervals of time. A blue-shift in PL peak position from 700 nm to 600 nm was observed for PS sample prepared at $I_d = 20 \text{ mA cm}^{-2}$ when exposed to ethanol vapors for 20 mins. However, the PL intensity remains the same upon exposure to ethanol. However, PS sample when exposed to H₂O-vapours exhibits a drastic reduction in PL intensity and a relatively

higher blue shift in PL from 700 nm to 560 nm as compared to ethanol-exposed PS sample for the same time of exposure. The PS sample shows lower response towards methanol gas as evident from a marginal reduction in PL intensity and blue shift in PL peak position from 700 nm to 690 nm respectively. Resistivity studies reveal that PS sample prepared at $I_d = 20 \text{ mA cm}^{-2}$ shows maximum and minimum sensitivity ($\Delta R/R$) values $\sim 90\%$ for both ethanol and humidity and $\sim 40\%$ for methanol gas respectively. With increase in current density, the response time in general decreases and the sensitivity value increases for PS samples upon exposure to ethanol and humidity in particular. The improved gas sensing properties are attributed to the formation of highly porous vertical layers separating macroscopic domains of nanoporous silicon. SEM, AFM and FTIR studies support the results as well.

CHAPTER 6

SUMMARY

6.1 SUMMARY

Monitoring and upkeep of the environment, for well being and health carries a very broad area comprise diverse factors like chemical, biological and human habitat. Historically, toxicity in the environment, infections and communicable disease has been at the center of environmental health including physical, sociological and psychological factors that may affect man's health and safety. Identification of toxicity, causative organisms, and routes of transmission, population at risk and the subsequent development of strategies to prevent transmission or treatment and cures for communicable diseases has dominated public health. Today, while chemical and biological hazards continue to be enormous public health issues, other hazards have emerged and demand attention. Concern for presence of chemicals and microorganisms in the atmosphere and their possible effect on human health has attained prominence. Some brief background of pioneering works in the area of PS thin films fabrication and characterization techniques have been presented in review of literature. Studies performed on PS formed on textured silicon substrates have revealed that semiconducting PS remains stable when exposed to oxygen ambient.

The project report begins with a description of the sample preparation procedure and it continues with the characterization techniques. For each characterization technique the basic theory is outlined, the setup is described and the measurement procedure is discussed. Accuracy and sensitivity requirements are addressed. It contains all the necessary information for the future repetition of this work.

We have also reported results of morphological, optical and electrical studies of Electrochemical deposited thin film of PS as monitored by SEM, AFM, FTIR and PL.

It can be concluded that quality PS nanocomposite thin films can be prepared by Electrochemical method. These films can be used for as efficient sensors for detection of toxic gas. These films are nanocrystalline in nature and behave like granular metallic crystallites embedded in a nonconducting medium. High sensitivity specificity and selectivity can be achieved by suitably PS at particular current density during synthesis. A stoichiometric composition HF: Ethanol (1:1) has been found to be suitable for the development of PS films for its possible application as ethanol gas and humidity sensors.

Microbiological sensors prepared from Fe doped polyaniline thin film vacuum deposited on porous silicon substrates have been found to exhibit excellent sensitivity towards the most commonly encountered microorganism (E.Coli) in water. The behavioral acceptance tests have shown that these sensors are highly specific and selective. The doping of Fe metal makes the polyaniline thin film sensor specific and selective for detection of E.coli. The current –voltage characteristics of the polyaniline sensor are affected by the presence of microorganism, which were used as a measure of the type and quantity of the microorganism. The sensitivity of the sensor has been observed to be high and the detection limit low. The stability, reproducibility and shelf life are good. The performance characteristics of the same have been established. The detection of such microorganism in water is essential to avoid infections in human beings. These polymeric sensors, therefore, have potential of being used in medical diagnostics, besides their use in monitoring the environment.

REFERENCES

REFERENCES

- [1]. Obisi, Stefano Ossicci, L. Pavesi, Surface science Reports 38 (2000) 1-126
- [2]. Lenward Seals and James L. Gole, Journal of Applied Physics volume 91, number 4, 15 February 2002
- [3]. Sanjay Chadane, Anisha Gokarna, Sv. Bhoraskar, Sensors and actuators B 92(2003) 1-5
- [4]. X.R. Zeng and T.M. Ko, Polymer, 39(1998) 1187.
- [5] L.T. Canham, Appl. Phys. Lett. 57 (1992) 1046.
- [6] V.S.Y. Lin, K. Motescharie, K.P.S. Dancil, M.J. Sailor, M.R. Ghadiri, Science 278 (1997) 840.
- [7] B. Hamilton, Semicond. Sci. Tech. 10 (1995) 1187.
- [8] V.V. Doan, M.J. Sailor, Science 256 (1992) 1791.
- [9] M.J. Sailor, J.L. Heinrich, J.M. Lauerhaas in: P.V. Kamat, D. Meisel (Eds.), Semiconductor Nanocrystals, Elsevier, New York 1996, p. 103.
- [10] M.P. Stewart, J.M. Buriak, Adv. Mater. 12 (2000) 859.
- [11] S.T. Lakshmi Kumar and P.K. Singh, J. Appl. Phys. 92 (2002) 3413.
- [12] O. Belmont, C. Faivre, D. Bellet, Y. Brechet, Thin Solid Films. 276 (1996) 219.
- [13] G. Kaltsas, A.G. Nassiopoulou, Microelec. Eng. 35 (1997) 397.
- [14] D. Papadimitriou, J. Bitsakis, J.M. Lopez-Villegas, J. Samitier, J.R. Morante, Thin Solid Films, 349 (1999) 293.

- [15] A.G. Cullis, L.T. Canham and P.D.J. Calcott, *J. Appl. Phys.* **82**, (1997) 909.
- [16] U. Gruning and A. Yelon, *Thin Solid Films* **255** (1995) 135.
- [17] G. Amato, N. Brunetto, *Materials Letters* **26** (1996) 295.
- [18] L.T. Canham, A.G. Cullis, C. Pickering, O.D. Dosser, T.I. Cox and P. Lynch, *Nature (London)*, **368** (1994) 133.
- [19] Han-Su Kim, Eric C. Zouzounis, and Ya-Hong Xie, *Appl. Phys. Lett.* **80** (2002) 2287.
- [20] J.M. Buriak and M.J. Allen, *J. Am. Chem. Soc.* **120** (1998) 1339.
- [21]. E.Yablonovitch, D.A.Allara, C.C.Chang, T.Grimmer and T.B.Bright,*Phys. Rev. Lett*, Vol. 57(2),pp.249-254(1986)
- [22]. A.Burghesi, A. Sassella., B. Pivac, L.Pavesi, *Lolid stat communication*, Vol87(1),(1993)
- [23]. Y.H.Seo, H.J.Lee, H.I.Jeon, D.H. Oh,K.S. Nahm,YH.Lee, E.K.Suh and H.Jlee, *Appl.Phys. Lett*, Vol.62 (15), pp1812-1814, April 12(1993)
- [24]. V.Petrova-Koch, T.muschik, A.Kux, B.K.Meyer, Fkoch and V.Lehman,*Appl. Phys. Lett*, Vol.61, pp.943-945(1992).
- [25] M. Guendouz, P. Joubert, and M. Sarret, *Mats. Sci & Eng. B* **69-70**, 43 (2000).
- [26] R.J. Martin Palma, L. Vazquez, P. Herrero, J.M. Martinez-Duart, M. Schnell, and S. Schaefer, *Optical Materials* **17**, 75 (2001).
- [27] H. Foll, M. Christophersen, J. Carstensen, and G. Hasse, *Mats. Sci. and Eng. R* **39**, 93 (2002).
- [28] V.K.Agrawals,*Physics toady*, 1(1988) 40.
- [29]. G.G.Roberts, *Sensors and Actuators*, 4(1975) 1380.
- [30]. J.Cha, Y.K.See, J.Lee and T.Chang, *Synthetic metals*, **117** (2001) 149.

- [31]. G.B.Khomutov, I.V.Beresneva, Y.A.Koksharov, I.L.Radchenko, I.V.Bykov,
R.V.Gainutdinov,S.N.Polyakov and D.L.Tolstikhina, Colloids Surf,A198(2002)509.
- [32]. Zknittl, OPTICS OF THIN films, (London:Johen Wiley & Sons)1976.
- [33]. R.Qian, J.Qiu and Dshen, Synthetic Metals18 (1987) 13.
- [34]. S.Hotta, Synthetic metals, 22(1988) 103.
- [35]. G.Kossmehl and G.Chatzi-theodorou Madromol. Chem. Rap. Commun, 2 (1981) 551.
- [36]. G.Kossmehl and G.Chatzi-theodorou, Mol. Cryst. Liq. Cryst., 83(1982)291.
- [37]. W.R. Salaneck, I.Lundstrom, B. Liedberg, M.Ahasan, R.Erlandsoon, P. Konradsoon, A.G. MacDiarmid and N.L.D.Somasiri, In "Electronic properties of conjugated Polymers and Related Compounds (Springer-Verlag, Berlin), 63(1985) 218.